Power Loss Analysis of Traditional PV Array Configurations Under Different Shading Conditions

Santosh B.S.S[*] [‡], Mohamed Thameem Ansari.M[**], Kantarao.P[***], Kusuma.G[****]

Department of Electrical Engineering, Annamalai University and Annamalai Nagar 608002, India[*].

Department of Electrical Engineering, SRKREC and Bhimavaram, India[*].

Department of Electrical Engineering, Annamalai University and Annamalai Nagar 608002, India[**].

Department of Electrical Engineering, SRKREC and Bhimavaram, India[***].

Department of Electrical Engineering, SRKREC and Bhimavaram, India[****].

(gangadharlakshmi555@gmail.com, ansariaueee@gmail.com, dr.pkantarao@gmail.com, dr.gkusuma9@gmail.com)

Corresponding author:[‡]B.S.S. Santosh; gangadharlakshmi555@gmail.com

Received: 29.04.2022 Accepted:02.06.2022

Abstract - Energy is an important criterion for economic progress nowadays. In general, more energy has been derived from fossil fuels in recent years. The world is using renewable energy sources to meet huge electricity needs due to scarcity and environmental risk issues. Photovoltaic (PV) energy is extensively used in the renewable energy sources because it is the most abundant energy source in nature, a simple energy conversion process. But solar cell capacity is very sensitive to non-uniform shading conditions. Also due to the unbalanced properties between the PV panels it produces a small amount of power and they cannot be operated with maximum energy value. One of the possible solutions is to mitigate this problem by connecting PV modules in different arrangements. In this article, seven traditional PV series topologies are: Series - S, Series Parallel - SP, Total Cross Tie - TCT, Bridge Link - BL, Honeycomb - HC, Triple Cross tie - TT, And Ladder - LD, analysed using a 6 × 6 PV range with different shading patterns using the SunPower SPR-76R-BLK-U PV module in the MATLAB/Simulink software. Theoretical analysis was performed by providing voltage, current and power values at each interval of bypass diode operation for each arrangement under all shading conditions and can be compared with simulation results. This analysis gives necessary design steps to arrange PV array under different shading regions. In all PV range configurations and under diagonal shading pattern, TCT offers outstanding performance in terms of highest maximum power of 2503 W with lowest mismatch loss of 1.37 %, low shade dispersion factor of 16.66 %, the fill factor and efficiency are 0.74 and 13.91 % respectively followed by TT, LD, HC, BL or SP and S.

Key words Maximum Power Point - MPP, Global Maximum Power Point - GMPP, Local Maximum Power Point - LMPP, Partial shading conditions - PSC, Mismatch power loss.

1. Introduction

Energy is a prerequisite for economic development and growth. With the fast- growing in industrialization and the drive to increase the economy, the world needs huge electricity [1]. In its endeavour to meet this demand mankind depends heavily on fossil fuels which is leads to substantial mining, an increase in global warming and, environmental pollution. The accelerating rate of extraction is culminating in an alarming depletion of fossil fuel reserves, and a surge in their price. Thus, it has become inevitable for the world to move to alternate resources for power generation [2]. According to 'International Energy Agency' (IEA) publication, non-conventional energy generation will continue to rise in importance as a primary source of electricity supply in the future. The usage of renewable energy can help save fossil fuels and money while also reducing pollution. Renewable energy is the topmost abundant source of energy in nature. India, being one of the world's fastest rising energy consumers, is investing heavily in the consumption and production of renewable energy, as well as ecological sustainability [3]. Solar power has increase in popularity among the public as a result of increased public awareness, government incentives, and technological developments that have considerably reduced the cost per watt. Despite technological developments, a few obstacles exist, including as low conversion efficiency, a high reliance on insolation, and other environmental aspects that decreases the output of solar PV systems. The PV panel generates nonlinear electrical characteristics. In order to get the better output from the PV module, it is always operated at the MPP and it is depending on the load. The system efficiency can be improved by using electrical tracking -to track the optimal operating point and mechanical tracking - to track the Sun. However, the power obtained from the PV system is generally observed to be less than that predicted or intended. The mismatch characteristics in the PV modules are the main cause of this disparity and they are Internal or external. Internal mismatches are caused by manufacturing methods, inadequate soldering bonding, or age, while outward mismatches are caused by partial shading. [4,5].

In a PV array, some of the cells or modules are shaded by trees, buildings, poles, birds, and moving clouds. Due to space limits, it is nearly impossible to avoid shading, and it is most commonly caused by adjacent constructions and buildings [6]. The electrical characteristics of shaded and unshaded panels differ, and this characteristic disparity grows as the illumination intensities differ. In practical operating conditions, there is a significant decrease in output power due to this mismatching. The reduction in power generated is a function of other factors like the location of shaded panels in the PV array, shading intensity, and, most importantly, PV array arrangement. In addition to this corrosion, snow and dust accumulated on the front facing of the panel greatly reduces the output power by hindering the insolation received by a PV panel and also its efficiency [7-9].

During uniform shading state, entire PV array operate at standard test conditions (STC) of 1kW/m^2 irradiance (G), 25^o C temperature (T) and generates unique electrical characteristics. Which results into no mismatching power loss, and PV system have a Single MPP on its output characteristics. The GMPP is a term used to describe the highest point on the Earth's surface. Conventional MPP trackers are used to trace this GMPP. [10-12].

Due to the partial shade of the PV module, the module current is reduced. This situation arises due to reverse bias operation of some of the PV cells in an array. Under shading condition, PV cells acts as a sink instead of source and voltage across it reached to its breakdown point leads to permanent damage like local hotspots, cracking’s on the cell, etc. The amount of reduction is determined by the shading intensity. Owing to mismatch losses, the amount of energy harvested from PV plants decreases (by about 20–25 percent).

According to the literature, the following steps [13] can be taken to mitigate the partial shading effects are: (i) connection of diodes across the each or group of modules [14], (ii) employing global peak power tracking methods (iii) implementing PV array configuration scheme.

PV systems represent multiple MPPs on its output characteristics under PSCs, are GMPP and the LMPP. Multiple MPPs can cause traditional MPPT techniques to fail, so soft computing-based MPPT methods are used. [15]. Metaheuristic techniques, fuzzy logic, artificial neural networks (ANN), and hybrid methods are all used to pursue the global peak. For tracking the global peak power, ANN and fuzzy methods require training and a large memory space. The metaheuristic algorithms are quite complicated and are based on a number of parameters. [16-21]. But, because these algorithms require a significant number of switches, sensors, sophisticated microcontrollers, and complex algorithms, their implementation in a PV system can increase system cost and complexity. Furthermore, the algorithms have reliability concerns when shading scenarios are dynamic or complex, as they sometimes track the false MPP.

Analyse the performance of various PV array configurations in [22] by comparing different parameters under row and column shading conditions and conclude that TCT array configuration is superior but the connecting scheme of this arrangement is having high redundancy. In [23], effects of PSCs on Array configuration, array size, and shading patterns are analysed using MATLAB M-code. Among all TCT configuration gives the optimum output. In [24], different PV configurations were analyzed by calculating shading loss, mismatch loss, and misleading loss and confirmed that the TCT configuration gives outstanding performance compared to others. In [25,26] evaluate the performance of various PV array topologies by modelling and simulation under several shading patterns and concluded that TCT connection scheme produces the maximum power with reduced mismatch power losses. The advanced techniques [27] to mitigate the partial shading effect are usage of multi tracker converters, micro converter - The power electronic converters with MPPT to each PV modules allow it to operate at maximum power. However, a large number of converters are required, which rises the system cost [28,29] and PV array reconfiguration.

Partial shading affect is more in series connected modules, whereas parallel connections are more adaptable under these situations. PV modules are primarily connected in series to form a string, later which is connected in parallel to form the most common connection method, Series-Parallel (SP). Researchers have proposed various different PV module connecting methods that improve the power generated in PSC. The shading condition has an impact on the power output of these connecting techniques (symmetrical or asymmetrical) [30].

From the literature, most of the researchers presents the mathematical analysis for TCT and HC configurations only. In this article, analysis is given for each configuration under all shading conditions in terms of operating modules, maximum voltage, maximum current and maximum power at each interval of string voltage. This analysis clearly gives the effect of bypass diode operation on the output power, identification of less utilized modules in an array, difficulties in maximum power point tracking and also it helps to design the PV array scheme, based on the location and objectives surrounding it by measuring shade dispersion factor. This metric is useful for obtaining maximum output power from the array.

The main objective of the work is analysing the various PV array schemes by deriving voltage and current equations. To identify the best topology that generates maximum output power under most of the shading conditions. Analysis has been performed for most of the shading conditions with different topologies. The TCT generates maximum power under most of the shading conditions compared to the existing topologies. A more detailed mathematical analysis is performed for different topologies and shading conditions.

This paper is ordered as follows: Section 2 clearly explains the analysis of PV Array Configurations in different shading patterns. Section 3 describes the performance assessment parameters. Section 4 presents the Comparative analysis of different PV array configurations along with simulation results.

2. PV Array Configurations and Illustration of Different Shading Patterns

For analysis purpose traditional PV Configurations are presented in this article. Different configurations, various shading patterns and performance assessment parameters as shown in Fig. 1. 6 × 6 matrix is used to model and simulation of above- mentioned PV array configurations. Simple single diode model [31] is used for PV module modelling and each module having 24 series connected cells and also each string is protected by bypass diodes. PV Configurations with different shading conditions are shown in Fig. 2.

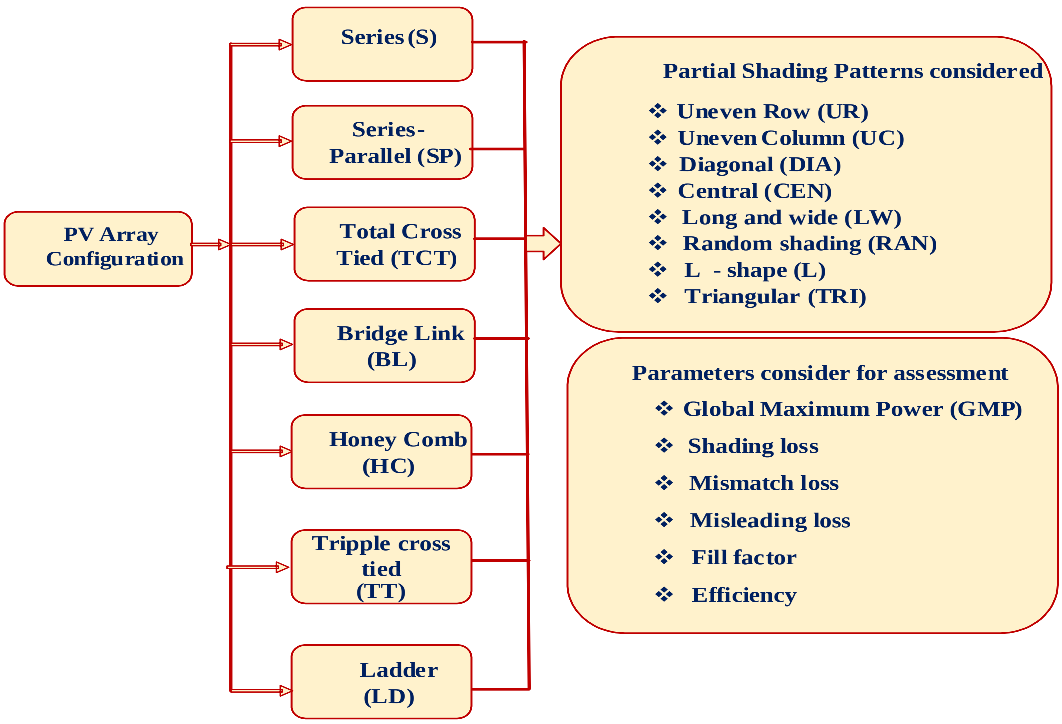

Fig. 1. Representation of different PV array Connection schemes, various shading patterns and performance assessment parameters.

SunPower SPR-76R-BLK-U PV module is used for the simulation to analyse the response of different PV arrayconfigurations and specifications are mentioned in Table 1.

Table 1. Specifications of SunPower SPR-76R-BLK-U PV module

S. no	Specifications	Values
1	Maximum Power (P_{max})	76.275 (W)
2	Open circuit voltage (V_{OC})	16.2 (V)
3	Short-circuit current (I_{SC})	6.02 (A)
4	Maximum power point voltage (V_{mpp})	13.5 (V)
5	Maximum power point current (I_{mpp})	5.65 (A)
6	Cells per module (N_{cell})	24
7	Temperature coefficient of Voc (K_V)	-0.379 (%/°C)
8	Temperature coefficient of Isc (K_I)	0.030997 (%/°C)
9	Diode ideality factor (a)	1.1181
10	Shunt resistance (R_p)	190.3046 (Ω)
11	Series resistance (R_s)	0.11329 (Ω)
12	Module area (A)	0.54 (m^2)

2.1 Series PV Array Configuration

It is the basic configuration as shown in Fig. 3, where all the PV Modules are connected in series. Simplicity, large voltage generation capability and low wiring loss are the major advantages. But it can be applicable for very small -scale PV systems because of current limitation of lowest shaded module on entire string. Which produces large power loss and generates multiple peaks in P-V characteristics, it leads to difficulty in MPP tracking. Where the total Array current (I) equal to module current or cell current and it can be represented in equ (7).

$$I = I_1 = I_2 = \cdots = I_{36} \quad (7)$$

Total array voltage is the sum of the individual module voltages and it can be represented in equ (8)

$$V = V_1 + V_2 + \cdots + V_{36} \quad (8)$$

Under uniform shading conditions all PV modules are operated at equal irradiance (G) and Temperature (T) conditions. Therefore, Single Peak occurs in the I-V and P-V characteristics, which is termed as Maximum Power Point (MPP). But during Partial shading conditions (PSC), multiple peaks occur due to non-linear characteristics of PV cell.

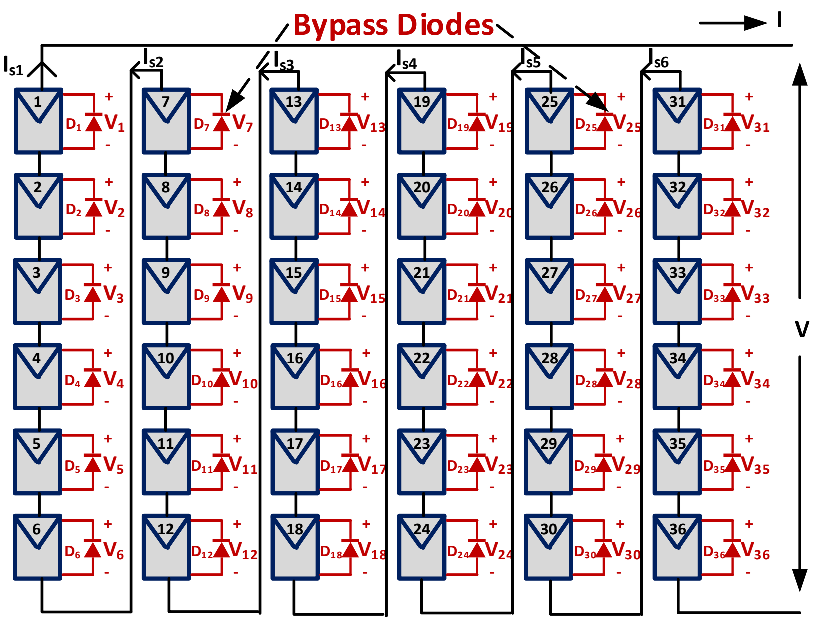

Fig. 3. Series PV Array Configuration

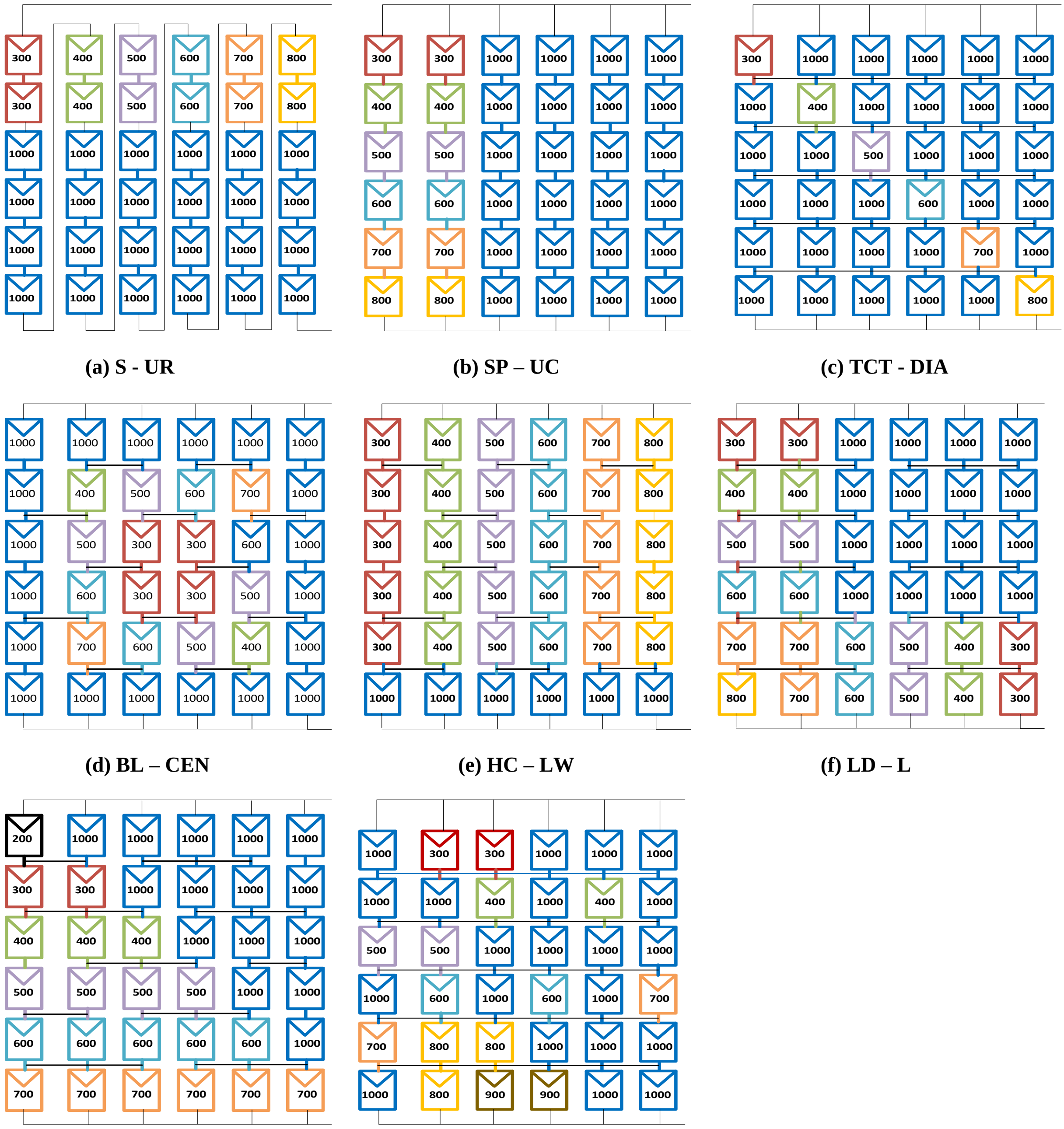

(a) S - UR **(b) SP – UC** **(c) TCT - DIA**

(d) BL – CEN **(e) HC – LW** **(f) LD – L**

(g) TT - TRI **(h) TCT – RAN**

Fig. 2. PV Configurations with different shading conditions

In a series PV array configuration, the lowest irradiance level of the PV module, which decides the array current, and non-linear characteristics of the PV cell or module, are the factors that produces the mismatch power losses. In order to satisfy the KVL across an array, a large reverse voltage developed across the shaded module to produce the short circuit current same as the unshaded module. Therefore, shaded module acts as a sink instead of source. Due to these local hot spots are generated with in the modules or cells, which damages the PV module. In order to Protect the PV modules, a diode is connected in ani-parallel to the PV module named as Bypass diode. Under PSC, reverse voltage across module forward biases the bypass diode. Then, portion of shaded panels short circuit current can be supplied through these diodes and these deviation of current path leads to occurrence of multiple peaks in the I-V and P-V Characteristics as shown in Fig. 4 and mathematical analysis of Array Voltage, Array Current and Array Power are mentioned in Table 2.

Table 2. Representation of Array Voltage, Array Current and Array Power under PSC for Series Configuration

Shading Pattern	**Array Current Interval**						
Uneven Row	$0.8I_m \le I \le I_m$	$0.7I_m \le I \le 0.8I_m$	$0.6I_m \le I \le 0.7I_m$	$0.5I_m \le I \le 0.6I_m$	$0.4I_m \le I \le 0.5I_m$	$0.3I_m \le I \le 0.4I_m$	$I \le 0.3I_m$
Operating Modules	3,4,5,6,9,10,11, 12,15,16,17,18, 21,22,23,24,27, 28,29,30,33,34, 35,36	31,32	25,26	19,20	13,14	7,8	1,2
PV Voltage	$24V_m$	$26V_m$	$28V_m$	$30V_m$	$32V_m$	$34V_m$	$36V_m$
PV Current	I_m	$0.8\ I_m$	$0.7\ I_m$	$0.6\ I_m$	$0.5\ I_m$	$0.4\ I_m$	$0.3\ I_m$
PV Power	**$24V_mI_m$**	$20.8\ V_mI_m$	$19.6\ V_mI_m$	$18\ V_mI_m$	$16\ V_mI_m$	$13.6\ V_mI_m$	$10.8\ V_mI_m$
Uneven Column	$0.8I_m \le I \le I_m$	$0.7I_m \le I \le 0.8I_m$	$0.6I_m \le I \le 0.7I_m$	$0.5I_m \le I \le 0.6I_m$	$0.4I_m \le I \le 0.5I_m$	$0.3I_m \le I \le 0.4I_m$	$I \le 0.3I_m$
Operating Modules	3,4,5,6,9,10,11, 12,15,16,17,18, 21,22,23,24,27, 28,29,30,33,34, 35,36.	31,32	25,26	19,20	13,14	7,8	1,2
PV Voltage	$24V_m$	$26V_m$	$28V_m$	$30V_m$	$32V_m$	$34V_m$	$36V_m$
PV Current	I_m	$0.8\ I_m$	$0.7\ I_m$	$0.6\ I_m$	$0.5\ I_m$	$0.4\ I_m$	$0.3\ I_m$
PV Power	**$24V_mI_m$**	$20.8\ V_mI_m$	$19.6\ V_mI_m$	$18\ V_mI_m$	$16\ V_mI_m$	$13.6\ V_mI_m$	$10.8\ V_mI_m$
Diagonal	$0.8I_m \le I \le I_m$	$0.7I_m \le I \le 0.8I_m$	$0.6I_m \le I \le 0.7I_m$	$0.5I_m \le I \le 0.6I_m$	$0.4I_m \le I \le 0.5I_m$	$0.3I_m \le I \le 0.4I_m$	$I \le 0.3I_m$
Operating Modules	2,3,4,5,6,7,9,10, 11,12,13,14,16, 17,18,19,20,21, 23,24,25,26,27, 28,29,31,32,33, 34,35,36.	36	29	22	15	8	1
PV Voltage	$30\ V_m$	$31\ V_m$	$32\ V_m$	$33\ V_m$	$34\ V_m$	$35\ V_m$	$36\ V_m$
PV Current	I_m	$0.8\ I_m$	$0.7\ I_m$	$0.6\ I_m$	$0.5\ I_m$	$0.4\ I_m$	$0.3\ I_m$
PV Power	**$30\ V_mI_m$**	$24.8\ V_mI_m$	$22.4\ V_mI_m$	$19.8\ V_mI_m$	$17\ V_mI_m$	$14\ V_mI_m$	$10.8\ V_mI_m$
Central	$0.7I_m \le I \le I_m$	$0.6I_m \le I \le 0.7I_m$	$0.5I_m \le I \le 0.6I_m$	$0.4I_m \le I \le 0.5I_m$	$0.3I_m \le I \le 0.4I_m$	$I \le 0.3I_m$	--
Operating Modules	1-6,7,12,13,18, 19,24,25,30, 31-36.	11,26	10,17,19,27	9,13,23,28	8,29	15,16,21,22	--
PV Voltage	$20\ V_m$	$22\ V_m$	$26\ V_m$	$30\ V_m$	$32\ V_m$	$36\ V_m$	--
PV Current	I_m	$0.7\ I_m$	$0.6\ I_m$	$0.5\ I_m$	$0.4\ I_m$	$0.3\ I_m$	--
PV Power	**$20\ V_mI_m$**	$15.4\ V_mI_m$	$15.6\ V_mI_m$	$15\ V_mI_m$	$12.8\ V_mI_m$	$10.8\ V_mI_m$	--
Random	$0.9I_m \le I \le I_m$	$0.7I_m \le I \le 0.8I_m$	$0.6I_m \le I \le 0.7I_m$	$0.5I_m \le I \le 0.6I_m$	$0.4I_m \le I \le 0.5I_m$	$0.3I_m \le I \le 0.4I_m$	$I \le 0.3I_m$
Operating Modules	1,2,4,6,8,15,16, 19,20,21,23,24 26-30, 31-33, 35,36.	11,12,17	5,34	10,22	3,9	14,26	7,10
PV Voltage	$21\ V_m$	$26\ V_m$	$28\ V_m$	$30\ V_m$	$32\ V_m$	$34\ V_m$	$36\ V_m$
PV Current	I_m	$0.8\ I_m$	$0.7\ I_m$	$0.6\ I_m$	$0.5\ I_m$	$0.4\ I_m$	$0.3\ I_m$
PV Power	**$21\ V_mI_m$**	$20.8\ V_mI_m$	$19.6\ V_mI_m$	$18\ V_mI_m$	$16\ V_mI_m$	$13.6\ V_mI_m$	$10.8\ V_mI_m$
Long & Wide	$0.8I_m \le I \le I_m$	$0.7I_m \le I \le 0.8I_m$	$0.6I_m \le I \le 0.7I_m$	$0.5I_m \le I \le 0.6I_m$	$0.4I_m \le I \le 0.5I_m$	$0.3I_m \le I \le 0.4I_m$	$I \le 0.3I_m$
Operating Modules	6,12,18,24,30, 36	31-35	25-29	19-23	13-17	7-11	1-5
PV Voltage	$6\ V_m$	$11\ V_m$	$16\ V_m$	$21\ V_m$	$26\ V_m$	$31\ V_m$	$36\ V_m$
PV Current	I_m	$0.8\ I_m$	$0.7\ I_m$	$0.6\ I_m$	$0.5\ I_m$	$0.4\ I_m$	$0.3\ I_m$
PV Power	$6\ V_mI_m$	$8.8\ V_mI_m$	$11.2\ V_mI_m$	$12.6\ V_mI_m$	**$13\ V_mI_m$**	$12.4\ V_mI_m$	$10.8\ V_mI_m$
L-shaped	$0.8I_m \le I \le I_m$	$0.7I_m \le I \le 0.8I_m$	$0.6I_m \le I \le 0.7I_m$	$0.5I_m \le I \le 0.6I_m$	$0.4I_m \le I \le 0.5I_m$	$0.3I_m \le I \le 0.4I_m$	$I \le 0.3I_m$
Operating Modules	13-16,19-22, 25-28, 31-34	6	5,11,12	4,10,17,18	3,9,23,24	2,8,29,30	1,2,35,36
PV Voltage	$16\ V_m$	$17\ V_m$	$20\ V_m$	$24\ V_m$	$28\ V_m$	$32\ V_m$	$36\ V_m$
PV Current	I_m	$0.8\ I_m$	$0.7\ I_m$	$0.6\ I_m$	$0.5\ I_m$	$0.4\ I_m$	$0.3\ I_m$
PV Power	**$16\ V_mI_m$**	$13.6\ V_mI_m$	$14\ V_mI_m$	$14.4\ V_mI_m$	$14\ V_mI_m$	$12.8\ V_mI_m$	$10.8\ V_mI_m$
Triangular	$\mathbf{0.7I_m \le I \le I_m}$	$\mathbf{0.6I_m \le I \le 0.7I_m}$	$\mathbf{0.5I_m \le I \le 0.6I_m}$	$\mathbf{0.4I_m \le I \le 0.5I_m}$	$\mathbf{0.3I_m \le I \le 0.4I_m}$	$\mathbf{0.2I_m \le I \le 0.3I_m}$	$\mathbf{I \le 0.2I_m}$
Operating Modules	7,13,14,19,20, 21,25,26,27,28, 31,32,33,34	6,12,18,24,30,36	5,11,17,23,29,35	4,10,16,22	3,9,15	2,8	1
PV Voltage	$15\ V_m$	$21\ V_m$	$26\ V_m$	$30\ V_m$	$33\ V_m$	$35\ V_m$	$36\ V_m$

PV Current	I_m	0.7 I_m	0.6 I_m	0.5 I_m	0.4 I_m	0.3 I_m	0.2 I_m
PV Power	15 V_mI_m	14.7 V_mI_m	**15.6 V_mI_m**	15 V_mI_m	13.2 V_mI_m	10.5 V_mI_m	6.4 V_mI_m

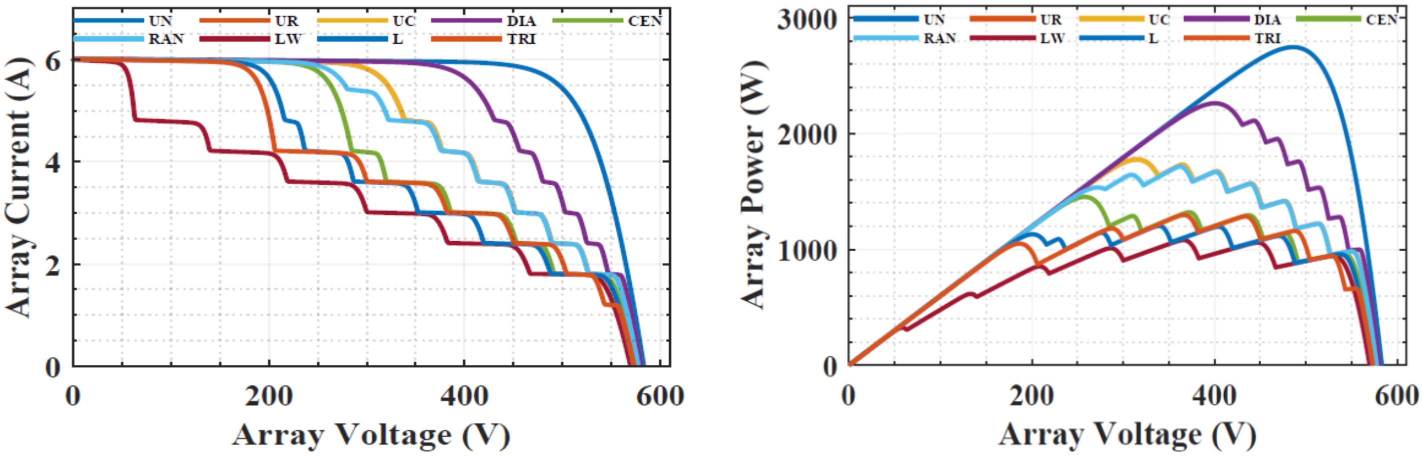

(a) (b)

Fig. 4. (a) I-V curves (b) P-V Curves of Series Configuration for different shading patterns

2.2 Series Parallel PV Array Configuration

It is the most commonly used configuration [26] as shown in Fig. 5. In this configuration primarily all the PV modules are connected in series fashion called as string in order to get required output voltage. Afterwards all the strings are connected in parallel to obtain desired output current. This configuration is equivalent to Parallelly connected series modules. The array Voltage and array current can be given as

$$V = \sum_{i=1}^{6} V_i = \sum_{i=7}^{12} V_i = \sum_{i=13}^{19} V_i = \sum_{i=19}^{24} V_i = \sum_{i=25}^{30} V_i = \sum_{i=31}^{36} V_i \quad (9)$$

$$I = I_{s1} + I_{s2} + I_{s3} + I_{s4} + I_{s5} + I_{s6} \quad (10)$$

In Fig. 5, blocking diodes are connected in series to each PV string in addition to by-pass diodes. In standalone PV systems during PSC or at night times current flows from the storage battery to the PV array. Under this condition blocking diodes are operated in a reverse bias state and protect the entire PV string from the reverse flow of current. The simulated I-V and P-V curves are shown in Fig. 6 and mathematical analysis of Array Voltage, Array Current and Array Power are mentioned in Table 3.

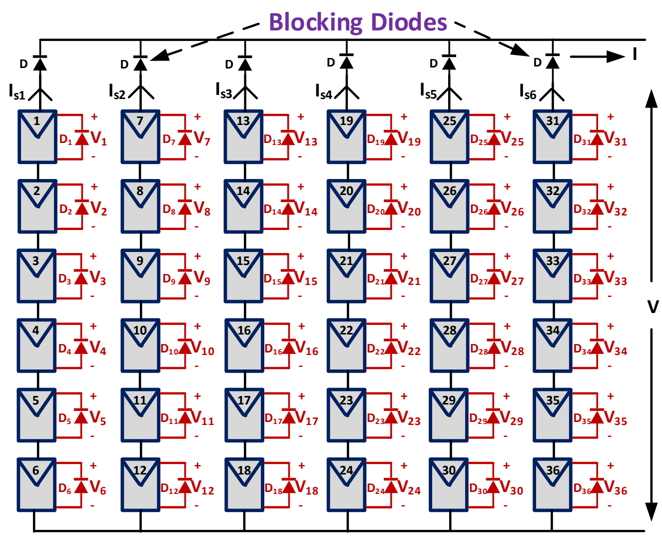

Fig. 5. Series - Parallel PV Array Configuration

Table 3. Representation of Array Voltage, Array Current and Array Power under PSC for Series - Parallel Configuration

Shading Pattern	**Array Voltage Interval**					
Uneven Row	$0 \leq V \leq 4V_m$				$4V_m \leq V \leq 6V_m$	
Operating Modules	3-6,9-12,15-18,21-24,27-30,33-36				1-2,7-8,13-14,19-20,25-26,31-32	
PV Voltage	$4V_m$				$6V_m$	
PV Current	$6I_m$				$3.3I_m$	
PV Power	**$24\ V_m I_m$**				$19.8\ V_m I_m$	
Uneven Column	$0 \leq V \leq V_m$	$V_m \leq V \leq 2V_m$	$2V_m \leq V \leq 3V_m$	$3V_m \leq V \leq 4V_m$	$4V_m \leq V \leq 5V_m$	$5V_m \leq V \leq 6V_m$
Operating Modules	6,12,18,24,30,36	5,11,17,23,29,35	4,10,16,22,28,34	3,9,15,21,27,33	2,8,14,20,26,32	1,7,13,19,25,31
PV Voltage	V_m	$2V_m$	$3V_m$	$4V_m$	$5V_m$	$6V_m$
PV Current	$5.6\ I_m$	$5.4\ I_m$	$5.2\ I_m$	$5\ I_m$	$4.8\ I_m$	$4.6\ I_m$
PV Power	$5.6\ V_m I_m$	$10.8\ V_m I_m$	$15.6\ V_m I_m$	$20\ V_m I_m$	$24\ V_m I_m$	**$27.6\ V_m I_m$**
Diagonal	$0 \leq V \leq 5V_m$			$5V_m \leq V \leq 6V_m$		
Operating Modules	2-6, 7,9-12,13,14,16-18, 19-21,23,24,25-28,30, 31-35			1,8,15,22,29,36		
PV Voltage	$5V_m$			$6V_m$		
PV Current	$6\ I_m$			$3.3\ I_m$		
PV Power	**$30\ V_m I_m$**			$19.8\ V_m I_m$		
Central	$0 \leq V \leq 2V_m$		$2V_m \leq V \leq 3V_m$	$3V_m \leq V \leq 4V_m$	$4V_m \leq V \leq 5V_m$	$5V_m \leq V \leq 6V_m$
Operating Modules	1,6,7,12,13,18,19,24,25,30,31,36		5,11,17,20,26,35	4,10,14,23,27,34	3,9,16,22,28,33	2,8,15,21,29,32
PV Voltage	$2\ V_m$		$3\ V_m$	$4\ V_m$	$5\ V_m$	$6\ V_m$
PV Current	$6\ I_m$		$4.6\ I_m$	$4.2\ I_m$	$3.6\ I_m$	$3.4\ I_m$
PV Power	$12\ V_m I_m$		$13.8\ V_m I_m$	$16.8\ V_m I_m$	$18\ V_m I_m$	**$20.4\ V_m I_m$**
Random	$0 \leq V \leq V_m$	$V_m \leq V \leq 2V_m$	$2V_m \leq V \leq 3V_m$	$3V_m \leq V \leq 4V_m$	$4V_m \leq V \leq 5V_m$	$5V_m \leq V \leq 6V_m$
Operating Modules	2,8,15,19,25,31	1,12,16,20,27,32	4,11,18,21,28,33	6,10,17,23,29,35	5,9,14,24,30,36	3,7,13,22,26,34
PV Voltage	V_m	$2\ V_m$	$3\ V_m$	$4\ V_m$	$5\ V_m$	$6\ V_m$
PV Current	$6\ I_m$	$5.8\ I_m$	$5.7\ I_m$	$5.4\ I_m$	$4.5\ I_m$	$2.8\ I_m$
PV Power	**6** $V_m I_m$	$11.6\ V_m I_m$	$17.1\ V_m I_m$	$21.6\ V_m I_m$	**$22.5\ V_m I_m$**	$16.8\ V_m I_m$
Long & Wide	$0 \leq V \leq V_m$			$V_m \leq V \leq 6V_m$		
Operating Modules	6,12,18,24,30,36			1-5,7-11,13-17,19-23,25-29,31-35		
PV Voltage	V_m			$6\ V_m$		
PV Current	$6\ I_m$			$3.3\ I_m$		
PV Power	$6\ V_m I_m$			**$19.8\ V_m I_m$**		
L-shaped	$0 \leq V \leq V_m$	$V_m \leq V \leq 2V_m$	$2V_m \leq V \leq 3V_m$	$3V_m \leq V \leq 4V_m$	$4V_m \leq V \leq 5V_m$	$5V_m \leq V \leq 6V_m$
Operating Modules	6,12,13,19,25,31	5,11,14,20,26,32	4,10,15,21,27,33	3,9,16,22,28,34	2,8,17,23,29,35	1,7,18,24,30,36
PV Voltage	V_m	$2\ V_m$	$3\ V_m$	$4\ V_m$	$5\ V_m$	$6\ V_m$
PV Current	$5.5\ I_m$	$5.4\ I_m$	$5.2\ I_m$	$5\ I_m$	$2.7\ I_m$	$2.4\ I_m$
PV Power	$5.5\ V_m I_m$	$10.8\ V_m I_m$	$15.6\ V_m I_m$	**$20\ V_m I_m$**	$13.5\ V_m I_m$	$14.4\ V_m I_m$
Triangular	**$0 \leq V \leq V_m$**	**$V_m \leq V \leq 2V_m$**	**$2V_m \leq V \leq 3V_m$**	**$3V_m \leq V \leq 4V_m$**	**$4V_m \leq V \leq 5V_m$**	**$5V_m \leq V \leq 6V_m$**
Operating Modules	6,7,13,19,25,31	5,12,14,20,26,32	4,11,18,21,27,33	3,10,17,24,28,34	2,9,16,23,30,35	1,8,15,22,29,36
PV Voltage	V_m	$2\ V_m$	$3\ V_m$	$4\ V_m$	$5\ V_m$	$6\ V_m$
PV Current	$5.7\ I_m$	$5.3\ I_m$	$4.8\ I_m$	$4.2\ I_m$	$3.5\ I_m$	$2.7\ I_m$
PV Power	$5.7\ V_m I_m$	$10.6\ V_m I_m$	$14.4\ V_m I_m$	$16.8\ V_m I_m$	**$17.5\ V_m I_m$**	$16.2\ V_m I_m$

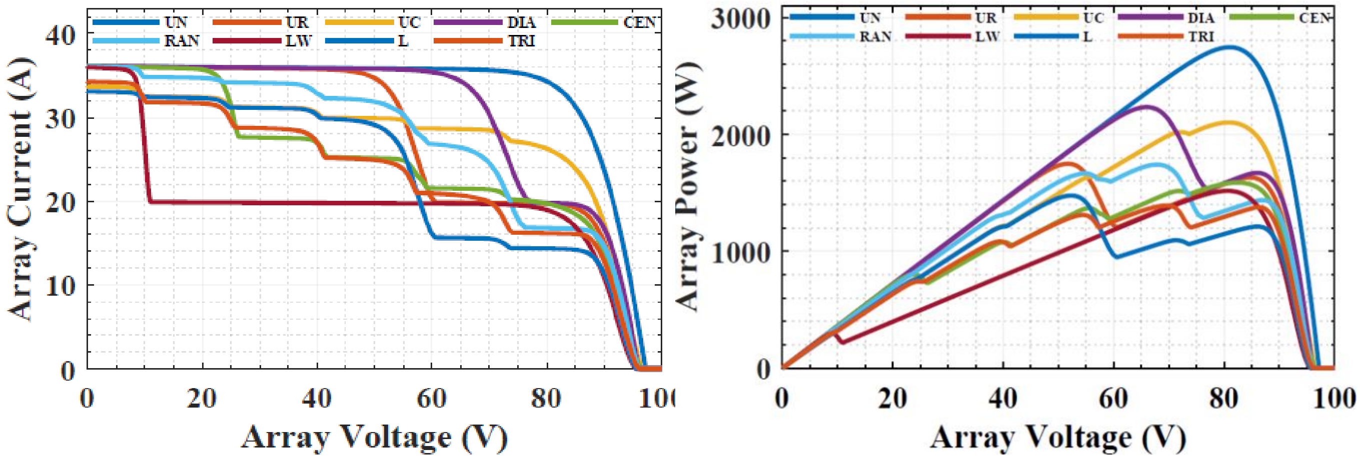

(a) (b)

Fig. 6. (a) I-V curves (b) P-V Curves of Series - Parallel Configuration for different shading patterns

2.3 Total-Cross-Tied (TCT) PV Array Configuration

In Series – Parallel Configuration, the number of series connected panels per string are more. This results in increasing the mismatching power loss but is lower than the Series configuration. This disadvantage can be overcome by initially connecting all the modules in parallel as rows and afterward are connected in series. This configuration is equivalent to Series connected Parallel modules. The 6×6 T-C-T PV array configuration as shown in Fig. 7. In every row the modules are connected in parallel, due to this we obtain low mismatch power loss compared to other configurations. But, because of the larger interconnections between the modules produces huge wiring loss and if there any problem occurs due to mismatch it is very difficult to identify the faulty module.

The Array Voltage is equal to sum of the voltages across the all rows and it can be expressed as

$$V = V_{R1} + V_{R2} + V_{R3} + V_{R4} + V_{R5} + V_{R6} \quad (11)$$

Where V_{R1}, V_{R2}, V_{R3}, V_{R4}, V_{R5}, V_{R6} are the corresponding row voltages and the voltage across each row is same as module voltage of particular row.

The Array current can be expressed as

$$I = I_{s1} + I_{s2} + I_{s3} + I_{s4} + I_{s5} + I_{s6} \quad (12)$$

The simulated I-V and P-V curves are shown in Fig. 8 and mathematical analysis of Array Voltage, Array Current and Array Power are mentioned in Table 4.

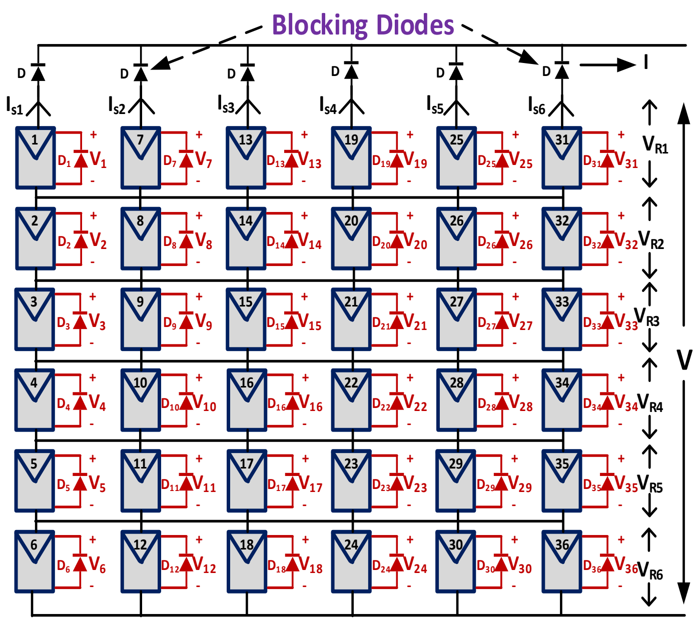

Fig. 7. TCT PV Array Configuration

Table 4. Representation of Array Voltage, Array Current and Array Power under PSC for TCT Configuration

Shading Pattern	Array Current Interval					
Uneven Row	$0 \le V \le 4V_m$			$4V_m \le V \le 6V_m$		
Operating Modules	3-6,9-12,15-18,21-24,27-30,33-36			1-2,7-8,13-14,19-20,25-26,31-32		
PV Voltage	$4 V_m$			$6 V_m$		
PV Current	$6 I_m$			$3.3 I_m$		
PV Power	**$24 V_m I_m$**			$19.8 V_m I_m$		
Uneven Column	$0 \le V \le V_m$	$V_m \le V \le 2V_m$	$2V_m \le V \le 3V_m$	$3V_m \le V \le 4V_m$	$4V_m \le V \le 5V_m$	$5V_m \le V \le 6V_m$
Operating Modules	6,12,18,24,30,36	5,11,17,23,29,35	4,10,16,22,28,34	3,9,15,21,27,33	2,8,14,20,26,32	1,7,13,19,25,31
PV Voltage	V_m	$2V_m$	$3 V_m$	$4 V_m$	$5 V_m$	$6 V_m$
PV Current	$5.6 I_m$	$5.4 I_m$	$5.2 I_m$	$5 I_m$	$4.8 I_m$	$4.6 I_m$
PV Power	$5.6 V_m I_m$	$10.8 V_m I_m$	$15.6 V_m I_m$	$20 V_m I_m$	$24 V_m I_m$	**$27.6 V_m I_m$**
Diagonal	$0 \le V \le V_m$	$V_m \le V \le 2V_m$	$2V_m \le V \le 3V_m$	$3V_m \le V \le 4V_m$	$4V_m \le V \le 5V_m$	$5V_m \le V \le 6V_m$
Operating Modules	6,12,18,24,30,36	5,11,17,23,29,35	4,10,16,22,28,34	3,9,15,21,27,33	2,8,14,20,26,32	1,7,13,19,25,31
PV Voltage	V_m	$2V_m$	$3 V_m$	$4 V_m$	$5 V_m$	$6 V_m$
PV Current	$5.8 I_m$	$5.7 I_m$	$5.6 I_m$	$5.5 I_m$	$5.4 I_m$	$5.3 I_m$
PV Power	$5.8 V_m I_m$	$11.4 V_m I_m$	$16.8 V_m I_m$	$22 V_m I_m$	$27 V_m I_m$	**$31.8 V_m I_m$**
Central	$0 \le V \le 2V_m$		$2V_m \le V \le 4V_m$		$4V_m \le V \le 6V_m$	
Operating Modules	1,7,13,19,25,31,6,12,18,24,30,36		2,8,14,20,26,32,5,11,17,23,29,35		3,9,15,21,27,33,4,10,16,22,28,34	
PV Voltage	$2 V_m$		$4 V_m$		$6 V_m$	
PV Current	$6 I_m$		$4.2 I_m$		$3.7 I_m$	
PV Power	$12 V_m I_m$		$16.8 V_m I_m$		**$22.2 V_m I_m$**	
Random	$0 \le V \le V_m$	$V_m \le V \le 2V_m$	$2V_m \le V \le 3V_m$	$3V_m \le V \le 4V_m$	$4V_m \le V \le 5V_m$	$5V_m \le V \le 6V_m$
Operating Modules	6,12,18,24,30,36	5,11,17,23,29,35	4,10,16,22,28,34	3,9,15,21,27,33	2,8,14,20,26,32	1,7,13,19,25,31
PV Voltage	V_m	$2V_m$	$3 V_m$	$4 V_m$	$5 V_m$	$6 V_m$
PV Current	$5.6 I_m$	$5.3 I_m$	$4.9 I_m$	$5 I_m$	$4.8 I_m$	$4.6 I_m$
PV Power	$5.6 V_m I_m$	$10.6 V_m I_m$	$14.7 V_m I_m$	$20 V_m I_m$	$24 V_m I_m$	**$27.6 V_m I_m$**
Long & Wide	$0 \le V \le 4V_m$			$4V_m \le V \le 6V_m$		
Operating Modules	6,12,18,24,30,36			1-5,7-11,13-17,19-23,25-29,31-35		
PV Voltage	V_m			$6 V_m$		
PV Current	$6 I_m$			$3.3 I_m$		
PV Power	$6 V_m I_m$			$19.8 V_m I_m$		
L-shaped	$0 \le V \le V_m$	$V_m \le V \le 2V_m$	$2V_m \le V \le 3V_m$	$3V_m \le V \le 4V_m$	$4V_m \le V \le 5V_m$	$5V_m \le V \le 6V_m$
Operating Modules	4,10,16,22,28,34	3,9,15,21,27,33	2,8,14,20,26,32	1,7,13,19,25,31	6,12,18,24,30,36	5,11,17,23,29,35
PV Voltage	V_m	$2V_m$	$3 V_m$	$4 V_m$	$5 V_m$	$6 V_m$
PV Current	$5.2 I_m$	$5 I_m$	$4.8 I_m$	$4.6 I_m$	$3.3 I_m$	$3.2 I_m$
PV Power	$5.2 V_m I_m$	$10 V_m I_m$	$14.4 V_m I_m$	$18.4 V_m I_m$	$16.5 V_m I_m$	**$19.2 V_m I_m$**
Triangular	$0 \le V \le V_m$	$V_m \le V \le 2V_m$	$2V_m \le V \le 4V_m$		$4V_m \le V \le 6V_m$	
Operating Modules	1,7,13,19,25,31	2,8,14,20,26,32	3,9,15,21,27,33, 6,12,18,24,30,36		4,10,16,22,28,34,5,11,17,23,29,35	
PV Voltage	V_m	$2 V_m$	$4 V_m$		$6 V_m$	
PV Current	$5.2 I_m$	$4.6 I_m$	$4.2 I_m$		$4 I_m$	
PV Power	$5.2 V_m I_m$	$9.2 V_m I_m$	$16.8 V_m I_m$		**$24 V_m I_m$**	

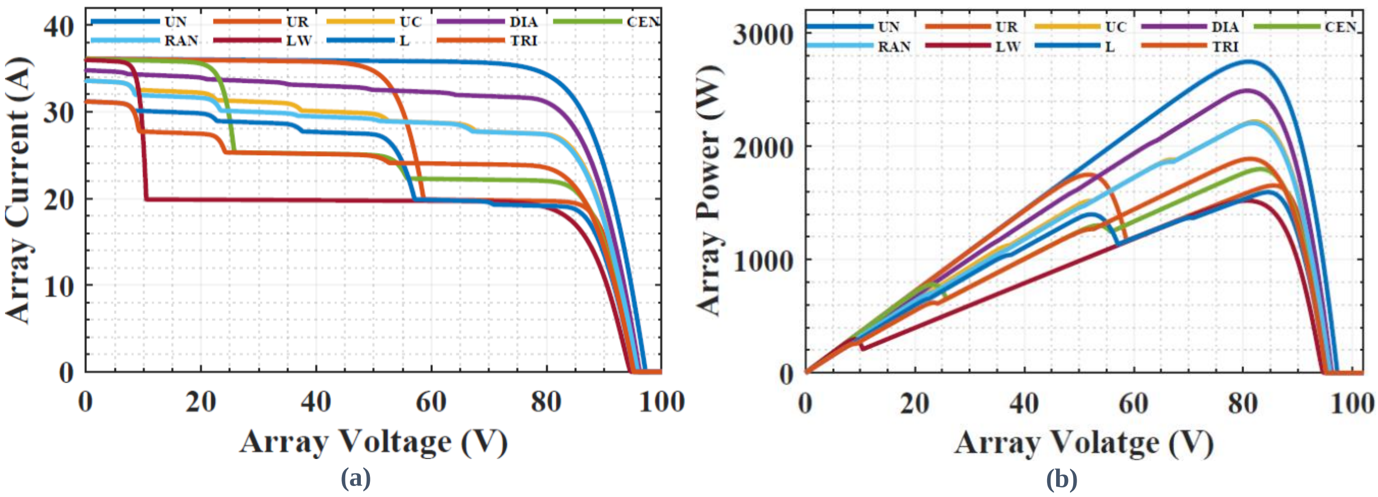

Fig. 8. (a) I-V curves (b) P-V Curves of TCT Configuration for different shading patterns

2.4 Bridge Link (BL) PV Array Configuration

The number of series connections between the modules in a string is the main reason to mismatch power loss. Series and Series- Parallel configurations offers more series connections which results larger the mismatch power loss. The alternate way to reduce these losses by connecting all modules in bridge rectifier fashion [32] as shown in Fig. 9. It generates low mismatch power loss when compared to SP and high with respect to TCT. Fault identification is flexible in BL configuration compared to TCT. It offers slightly wide operating time and less susceptible to electrical disturbance.

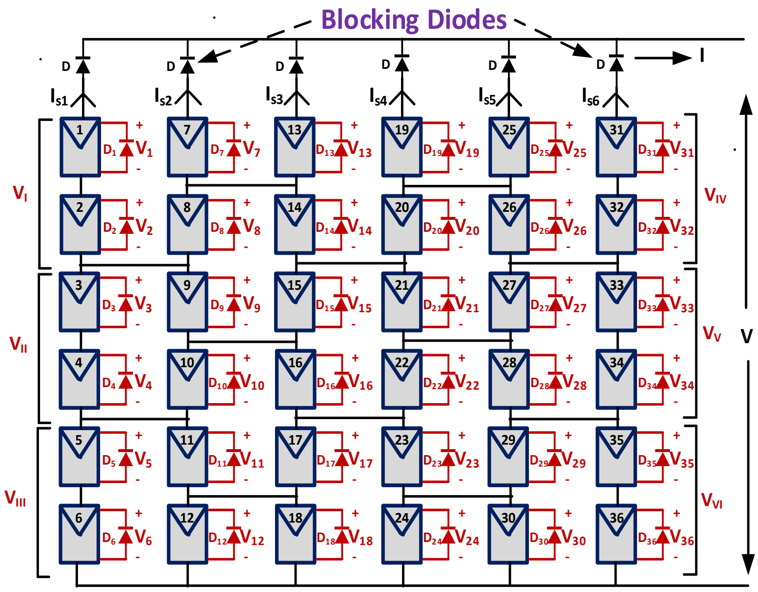

Fig. 9. BL PV Array Configuration

The Array Voltage and Currents can be expresses as

$V = V_I + V_{II} + V_{III} = V_{IV} + V_V + V_{VI}$ (13)

Where $V_I = V_{12} = V_7 + V_8$; $V_{II} = V_{34} = V_9 + V_{10}$; $V_{III} = V_{56} = V_{11} + V_{12}$; $V_{IV} = V_{3132} = V_{25} + V_{26}$; $V_V = V_{3334} = V_{27} + V_{28}$; $V_{VI} = V_{3536} = V_{29} + V_{30}$

and $I = I_{s1} + I_{s2} + I_{s3} + I_{s4} + I_{s5} + I_{s6}$ (14)

The simulated I-V and P-V curves are shown in Fig. 10 and mathematical analysis of Array Voltage, Array Current and Array Power are mentioned in Table 5.

Table 5. Representation of Array Voltage, Array Current and Array Power under PSC for BL Configuration

Shading Pattern	**Array Current Interval**					
Uneven Row	$0 \le V \le 4V_m$			$4V_m \le V \le 6V_m$		
Operating Modules	3-6,9-12,15-18,21-24,27-30,33-36			1-2,7-8,13-14,19-20,25-26,31-32		
PV Voltage	4 V_m			6 V_m		
PV Current	6 I_m			3.3 I_m		
PV Power	**24 $V_m I_m$**			19.8 $V_m I_m$		
Uneven Column	$0 \le V \le V_m$	$V_m \le V \le 2V_m$	$2V_m \le V \le 3V_m$	$3V_m \le V \le 4V_m$	$4V_m \le V \le 5V_m$	$5V_m \le V \le 6V_m$
Operating Modules	6,12,18,23,24,28-30, 33-36	5,11,16,21,23,24, 26,28-30,31-36	4,10,16,17,21-24,26-30,31-36	3,9,14,15,19-22,25-29,31-36	2,8,14,15,19-22,25-29,31-34	1,7,13,19,20,25-28,31-34
PV Voltage	V_m	2V_m	3 V_m	4 V_m	5 V_m	6 V_m
PV Current	5.6 I_m	5.4 I_m	5.2 I_m	5 I_m	4.8 I_m	4.6 I_m
PV Power	5.6 $V_m I_m$	10.8 $V_m I_m$	15.6 $V_m I_m$	20 $V_m I_m$	24 $V_m I_m$	**27.6 $V_m I_m$**
Diagonal	$0 \le V \le 5V_m$			$5V_m \le V \le 6V_m$		
Operating Modules	2-6, 7,9-12,13,14,16-18, 19-21,23,24,25-28,30, 31-35			1,8,15,22,29,36		
PV Voltage	5V_m			6V_m		
PV Current	6 I_m			3.3 I_m		
PV Power	**30 $V_m I_m$**			19.8 $V_m I_m$		
Central	$0 \le V \le 2V_m$		$2V_m \le V \le 4V_m$		$4V_m \le V \le 5V_m$	$5V_m \le V \le 6V_m$
Operating Modules	1,2,5,6,7,12,13,18,19,24,25,30,31-36		1-6,10,17,20,27,31-36		1-6,9,16,21,28,31-36	1-6,8,15,22,29,31-36
PV Voltage	2 V_m		4 V_m		5 V_m	6 V_m
PV Current	6 I_m		4.1 I_m		3.6 I_m	3.4 I_m
PV Power	12 $V_m I_m$		16.4 $V_m I_m$		18 $V_m I_m$	**20.4 $V_m I_m$**
Random	$0 \le V \le V_m$	$V_m \le V \le 2V_m$	$2V_m \le V \le 3V_m$	$3V_m \le V \le 4V_m$	$4V_m \le V \le 5V_m$	$5V_m \le V \le 6V_m$
Operating Modules	1,2,8,15,21,27,33	1,2,6,12,18,23,29, 35,36	1,2,4,10,17,24, 30,35,36	1,2,5,11,14,19,2 5,31	1,2,5,7,13,22,28 ,34	3,9,13,20,26,31, 32
PV Voltage	V_m	2V_m	3 V_m	4 V_m	5 V_m	6 V_m
PV Current	6 I_m	5.7 I_m	5.3 I_m	4.9 I_m	4.7 I_m	4.2 I_m
PV Power	6 $V_m I_m$	11.4 $V_m I_m$	15.9 $V_m I_m$	19.6 $V_m I_m$	23.5 $V_m I_m$	**25.2 $V_m I_m$**
Long & Wide	$0 \le V \le V_m$			$V_m \le V \le 6V_m$		
Operating Modules	6,12,18,24,30,36			1-5,7-11,13-17,19-23,25-29,31-35		
PV Voltage	V_m			6 V_m		
PV Current	6 I_m			3.3 I_m		
PV Power	6 $V_m I_m$			**19.8 $V_m I_m$**		
L-shaped	$0 \le V \le V_m$	$V_m \le V \le 2V_m$	$2V_m \le V \le 3V_m$	$3V_m \le V \le 4V_m$	$4V_m \le V \le 5V_m$	$5V_m \le V \le 6V_m$
Operating Modules	6,11,16,21,22,26,27,28, 31-34	4,9,14,19,21,22,25, 26,27,28,31-34	2,8,15,20,25-28,31-34	1,3,5,7,10,13-16,19-22,25-29,31-34	1,3,5,7,10,13,19, 25,31-34	5,12,17-18,23-24,29-30,35-36
PV Voltage	V_m	2V_m	3 V_m	4 V_m	5 V_m	6 V_m
PV Current	5.5 I_m	5.1 I_m	4.8 I_m	4.6 I_m	3.4 I_m	3.2 I_m
PV Power	5.5 $V_m I_m$	10.2 $V_m I_m$	14.4 $V_m I_m$	18.4 $V_m I_m$	17 $V_m I_m$	**19.2 $V_m I_m$**
Triangular	**$0 \le V \le V_m$**	**$V_m \le V \le 2V_m$**	**$2V_m \le V \le 3V_m$**	**$3V_m \le V \le 4V_m$**	**$4V_m \le V \le 5V_m$**	**$5V_m \le V \le 6V_m$**
Operating Modules	2,7,13,19,25-26,31-34	4,9,14,19-20,25-28,31-34	6,11,16,21,25-27,31-34	5,11,18,23,28,31-34	3,10,17,24,30,35	1,8,15,22,29,36
PV Voltage	V_m	2V_m	3 V_m	4 V_m	5 V_m	6 V_m
PV Current	5.3 I_m	4.9 I_m	4.7 I_m	4.5 I_m	3.9 I_m	2.7 I_m
PV Power	5.3 $V_m I_m$	9.8 $V_m I_m$	14.1 $V_m I_m$	18 $V_m I_m$	**19.5 $V_m I_m$**	16.2 $V_m I_m$

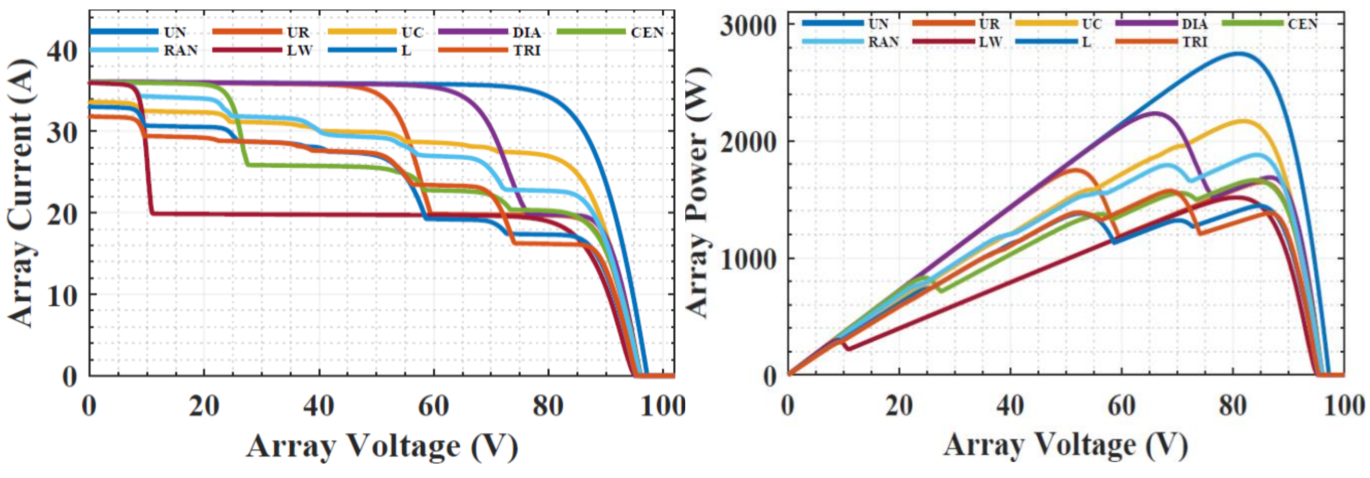

(a) (b)

Fig. 10. (a) I-V curves (b) P-V Curves of BL Configuration for different shading pattern

2.5 Honey Comb (HC) PV Array Configuration

The demerits of Series and Series-Parallel PV array topology can also overwhelm by connecting the PV modules similar to the hexagon shape of the honeycomb architecture [32] as shown in Fig. 11 It gives better output under asymmetrical array size or when number of rows of the modules is lower than the number of parallel strings receiving same irradiance. HC configuration has larger number of series connected modules per string compared to TCT and BL and a smaller number of series connected modules per string when compared to SP. So, larger the mismatch power loss compared to TCT and BL but lower with respect to SP configuration.

The Array Voltage and Currents can be expresses as

$$V = V_I + V_{II} + V_{III} + V_{IV} = V_V + V_{VI} + V_{VII} + V_{VIII} \quad (15)$$

Where $V_I = V_1 = V_7$; $V_{II} = V_{234} = V_8 + V_9 + V_{10}$; $V_{III} = V_5 = V_{11}$; $V_{IV} = V_6 = V_{12}$;$V_V = V_{31} = V_{25}$; $V_{VI} = V_{323334} = V_{26} + V_{27} + V_{28}$; $V_{VII} = V_{35} = V_{29}$; $V_{VIII} = V_{36} = V_{30}$;

and

$$I = I_{s1} + I_{s2} + I_{s3} + I_{s4} + I_{s5} + I_{s6} \quad (16)$$

The simulated I-V and P-V curves are shown in Fig. 12 and mathematical analysis of Array Voltage, Array Current and Array Power are mentioned in Table 6.

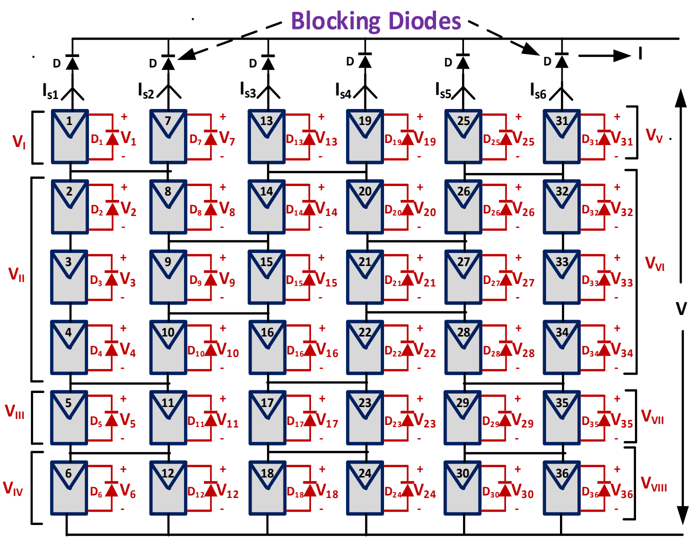

Fig. 11. HC PV Array Configuration

Table 6. Representation of Array Voltage, Array Current and Array Power under PSC for HC Configuration

Shading Pattern	Array Current Interval					
Uneven Row	$0 \le V \le 4V_m$			$4V_m \le V \le 6V_m$		
Operating Modules	3-6,9-12,15-18,21-24,27-30,33-36			1-2,7-8,13-14,19-20,25-26,31-32		
PV Voltage	$4\ V_m$			$6\ V_m$		
PV Current	$6\ I_m$			$3.3\ I_m$		
PV Power	**$24\ V_m I_m$**			$19.8\ V_m I_m$		
Uneven Column	$0 \le V \le V_m$	$V_m \le V \le 2V_m$	$2V_m \le V \le 3V_m$	$3V_m \le V \le 4V_m$	$4V_m \le V \le 5V_m$	$5V_m \le V \le 6V_m$
Operating Modules	6,12,16-18,20-24,25,27-30,31-36	5,11,16-18,20-24,25-30,31-36	4,10, 16-18,20-24,25-30,31-36	4,9,10,15,20-22, 25-30,31-36	2,3,8,13,14,19, 25-30,31-36	1,7,14,22,25-26,31-32,
PV Voltage	V_m	$2V_m$	$3\ V_m$	$4\ V_m$	$5\ V_m$	$6\ V_m$
PV Current	$5.6\ I_m$	$5.4\ I_m$	$5.2\ I_m$	$5.1\ I_m$	$4.8\ I_m$	$4.6\ I_m$
PV Power	$5.6\ V_m I_m$	$10.8\ V_m I_m$	$15.6\ V_m I_m$	$20.4\ V_m I_m$	$24\ V_m I_m$	**$27.6\ V_m I_m$**
Diagonal	$0 \le V \le 2V_m$		$2V_m \le V \le 3V_m$	$3V_m \le V \le 4V_m$	$4V_m \le V \le 5V_m$	$5V_m \le V \le 6V_m$
Operating Modules	2-6,10-12,16-18,20,21,23,24,25-28,31-34		2-4,11,12,17,18,20, 21,25-28,30, 31-34,36	2-4,9,15,19,25, 26,31-34	2-4,8,13,19, 25-26,31	1,7,14,22,29,35
PV Voltage	$2V_m$		$3\ V_m$	$4\ V_m$	$5\ V_m$	$6\ V_m$
PV Current	$6\ I_m$		$5.8\ I_m$	$5.5\ I_m$	$5.4\ I_m$	$4.6\ I_m$
PV Power	$12\ V_m I_m$		$17.4\ V_m I_m$	$22\ V_m I_m$	$27\ V_m I_m$	**$27.6\ V_m I_m$**
Central	Operating Modules		Operating Modules	Operating Modules	Operating Modules	Operating Modules
Operating Modules	1,6,7,12,13,18,19,24,25,30,31,36		5,11,16,17,20,23,26, 28,32,33,34	2-4,8,10,14,16, 20,25,27,32-34	2-4,10,14,21,27, 32,33	2-4,9,15,22,27,35
PV Voltage	$2V_m$		$3\ V_m$	$4\ V_m$	$5\ V_m$	$6\ V_m$
PV Current	$6\ I_m$		$4.7\ I_m$	$4.3\ I_m$	$4.3\ I_m$	$3.7\ I_m$
PV Power	$12\ V_m I_m$		$14.1\ V_m I_m$	$17.2\ V_m I_m$	$21.5\ V_m I_m$	**$22.2\ V_m I_m$**
Random	$0 \le V \le V_m$	$V_m \le V \le 2V_m$	$2V_m \le V \le 3V_m$	$3V_m \le V \le 4V_m$	$4V_m \le V \le 5V_m$	$5V_m \le V \le 6V_m$
Operating Modules	6,12,16,20,21,25,27 ,31-33	2,4,9,15,20,21,2 5,27,31-33	2,4,15,17,18,20,21, 23,24,25,27,29,30, 31-33,35,36	5,11,17,18,23, 24,28-30, 31-33,35,36	3,8,14,22,29,30,35, 36	1,7,13,19,26,34
PV Voltage	V_m	$2V_m$	$3\ V_m$	$4\ V_m$	$5\ V_m$	$6\ V_m$
PV Current	$5.8\ I_m$	$5.5\ I_m$	$5.4\ I_m$	$5.3\ I_m$	$4.5\ I_m$	$4\ I_m$
PV Power	$5.8\ V_m I_m$	$11\ V_m I_m$	$16.2\ V_m I_m$	$21.2\ V_m I_m$	$22.5\ V_m I_m$	**$24\ V_m I_m$**
Long & Wide	$0 \le V \le V_m$			$V_m \le V \le 6V_m$		
Operating Modules	6,12,18,24,30,36			1-5,7-11,13-17,19-23,25-29,31-35		
PV Voltage	V_m			$6\ V_m$		
PV Current	$6\ I_m$			$3.3\ I_m$		
PV Power	$6\ V_m I_m$			**$19.8\ V_m I_m$**		
L-shaped	$0 \le V \le V_m$	$V_m \le V \le 2V_m$	$2V_m \le V \le 3V_m$	$3V_m \le V \le 4V_m$	$4V_m \le V \le 5V_m$	$5V_m \le V \le 6V_m$
Operating Modules	6,12,16,20-22,25-28,31-34	3,9,15,20-22,25-28,31-34	3,9,13,14,19-22,25-28,31-34	1,7,13,14,19-22,25-28,31-34	5,6,11,12,17,18, 23,24,29,30,35,36	2,10,17,18, 23,24,29,30,35 ,36
PV Voltage	V_m	$2\ V_m$	$3\ V_m$	$4\ V_m$	$5\ V_m$	$6\ V_m$
PV Current	$5.5\ I_m$	$5.1\ I_m$	$4.\ 9\ I_m$	$4.6\ I_m$	$3.3\ I_m$	$3.2\ I_m$
PV Power	$5.5\ V_m I_m$	$10.2\ V_m I_m$	$14.7\ V_m I_m$	$18.4\ V_m I_m$	$16.5\ V_m I_m$	**$19.2\ V_m I_m$**
Triangular	$0 \le V \le V_m$	$V_m \le V \le 2V_m$	$2V_m \le V \le 3V_m$	$3V_m \le V \le 4V_m$	$4V_m \le V \le 5V_m$	$5V_m \le V \le 6V_m$
Operating Modules	1,7,13,14,16,19-21,25-27,31-34	6,12,13,14,16, 19-21,25-27,31-34	4,6,8,12,18,19-21,25-28,31-34	5,11,18,24,25-28,31-34	3,10,17,23,29,35	2,9,15,22,30, 36
PV Voltage	V_m	$2\ V_m$	$3\ V_m$	$4\ V_m$	$5\ V_m$	$6\ V_m$
PV Current	$5.2\ I_m$	$4.9\ I_m$	$4.5\ I_m$	$4.6\ I_m$	$3.3\ I_m$	$3.2\ I_m$
PV Power	$5.2\ V_m I_m$	$9.8\ V_m I_m$	$13.5\ V_m I_m$	$18.4\ V_m I_m$	$16.5\ V_m I_m$	**$19.2\ V_m I_m$**

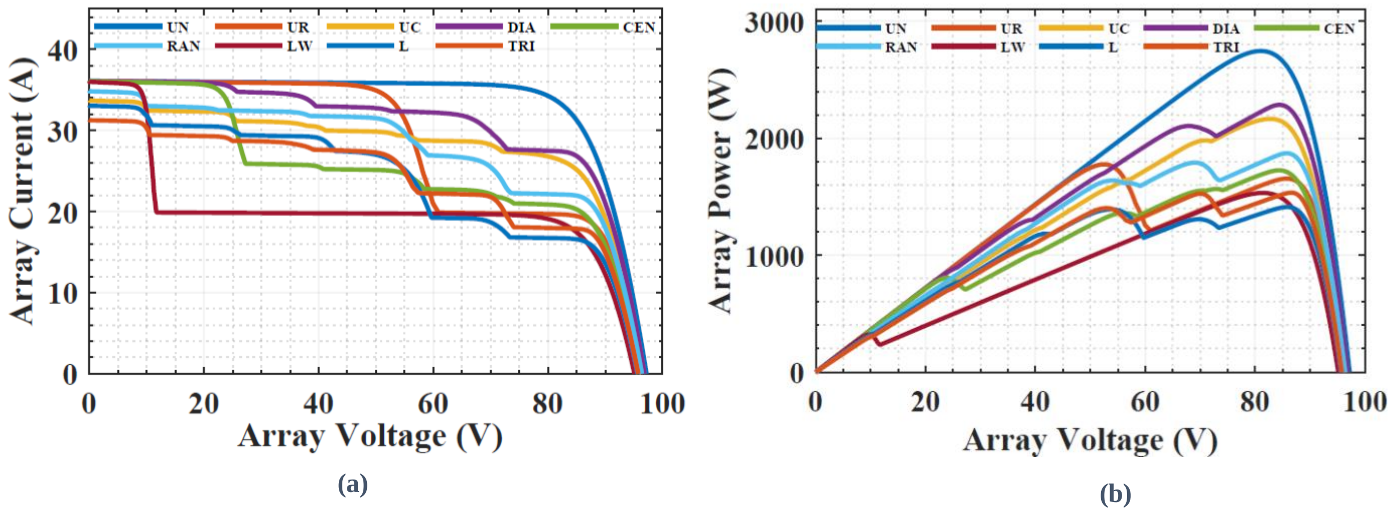

Fig. 12. (a) I-V curves (b) P-V Curves of HC Configuration for different shading patterns

2.6 Triple-Cross-Tied (TT) PV Array Configuration

It is the modified version of BL or HC configuration. Here, 3 modules are connected followed by gap afterwards and also it can be viewed as a cross tie configuration because of linking of strings with cross ties as shown in Fig. 13 The connecting pattern of TT configuration is inspired by flights of staircase [32].

The Array Voltage and Currents can be expresses as

$$V = V_I + V_{II} + V_{III} + V_{IV} + V_V = V_{VI} + V_{VII} + V_{VIII} + V_{IX} + V_x \quad (17)$$

Where $V_I = V_1 = V_7$; $V_{II} = V_2 = V_8$; $V_{III} = V_3 + V_4 = V_9 + V_{10}$; $V_{IV} = V_5 = V_{11}$; $V_V = V_6 = V_{12}$; $V_{VI} = V_{3132} = V_{25} + V_{26}$; $V_{VII} = V_{33} = V_{27}$;
$V_{VIII} = V_{3435} = V_{28} + V_{29}$; $V_{VIX} = V_{36} = V_{30}$; and

$$I = I_{s1} + I_{s2} + I_{s3} + I_{s4} + I_{s5} + I_{s6} \quad (18)$$

The simulated I-V and P-V curves are shown in Fig. 14 and mathematical analysis of Array Voltage, Array Current and Array Power are mentioned in Table 7.

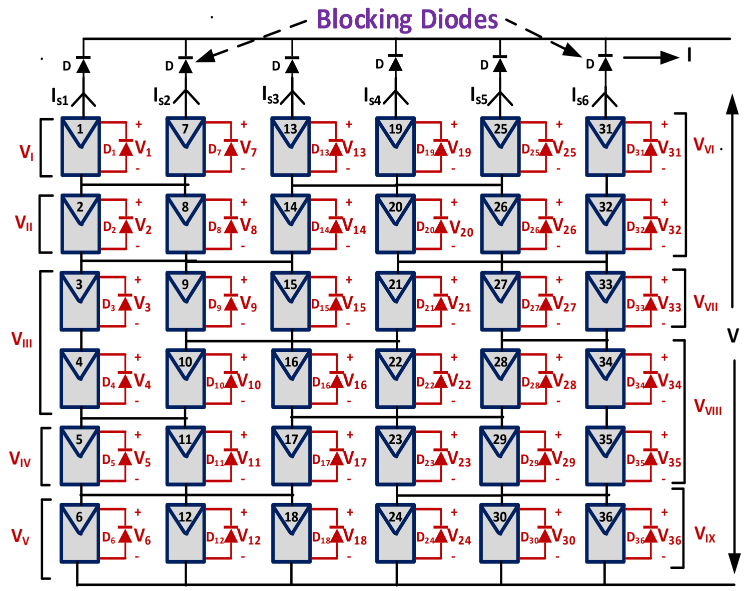

Fig. 13. TT PV Array Configuration

Table 7. Representation of Array Voltage, Array Current and Array Power under PSC for TT Configuration

Shading Pattern	**Array Current Interval**					
Uneven Row	$0 \le V \le 4V_m$			$4V_m \le V \le 6V_m$		
Operating Modules	3-6,9-12,15-18,21-24,27-30,33-36			1-2,7-8,13-14,19-20,25-26,31-32		
PV Voltage	$4\ V_m$			$6\ V_m$		
PV Current	$6\ I_m$			$3.3\ I_m$		
PV Power	**$24\ V_m I_m$**			$19.8\ V_m I_m$		
Uneven Column	$0 \le V \le V_m$	$V_m \le V \le 2V_m$	$2V_m \le V \le 3V_m$	$3V_m \le V \le 4V_m$	$4V_m \le V \le 5V_m$	$5V_m \le V \le 6V_m$
Operating Modules	6,12,17,18,23,24, 29,30,34-36	5,11,16,17,22-24,28-30,34-36	4,9,10,15-17,20,22-24,26-30,31-36	3,9,10,15,17,20, 21,26-28,31-36	2,3,8,13,14,17,19 -21,25-27,31-35	1,7,13,14,19-21,25-28,31-35
PV Voltage	V_m	$2V_m$	$3\ V_m$	$4\ V_m$	$5\ V_m$	$6\ V_m$
PV Current	$5.6\ I_m$	$5.4\ I_m$	$5.2\ I_m$	$5\ I_m$	$4.9\ I_m$	$4.6\ I_m$
PV Power	$5.6\ V_m I_m$	$10.8\ V_m I_m$	$15.6\ V_m I_m$	$20\ V_m I_m$	$24.5 V_m I_m$	**$27.6\ V_m I_m$**
Diagonal	$0 \le V \le V_m$	$V_m \le V \le 2V_m$	$2V_m \le V \le 3V_m$	$3V_m \le V \le 4V_m$	$4V_m \le V \le 5V_m$	$5V_m \le V \le 6V_m$
Operating Modules	3-6,10,12,17,18, 24,30,36	4-6,10,12,16-18,21 24,27,29,30,34-36	4-6,10-12,15-16, 20,22,26-28,31-35	2,8,9,13-15,19-21,25-28,31-35	2,8,13,14,19-21, 25-28,31-35	1,7,13,14,19-21,25-28,31-34
PV Voltage	V_m	$2V_m$	$3\ V_m$	$4\ V_m$	$5\ V_m$	$6\ V_m$
PV Current	$5.8\ I_m$	$5.7\ I_m$	$5.6\ I_m$	$5.5\ I_m$	$5.4\ I_m$	$5.3 I_m$
PV Power	$5.8\ V_m I_m$	$11.4\ V_m I_m$	$16.8\ V_m I_m$	$22\ V_m I_m$	$27\ V_m I_m$	**$31.8\ V_m I_m$**
Central	$0 \le V \le 2V_m$		$2V_m \le V \le 4V_m$		$4V_m \le V \le 5V_m$	$5V_m \le V \le 6V_m$
Operating Modules	1,6,7,12,13,18,19,24,25,30,31,32,36		3-5,9,11,15,16,21,22,27,28,31-35		2,3,8,10,14,20,21 ,26,31,32,34,35	3,4,8,10,14,17,20, 23,26,29,34,35
PV Voltage	$2V_m$		$4V_m$		$5\ V_m$	$6\ V_m$
PV Current	$6\ I_m$		$3.9\ I_m$		$4.2\ I_m$	$3.9\ I_m$
PV Power	$12\ V_m I_m$		$15.6\ V_m I_m$		$21\ V_m I_m$	**$23.4\ V_m I_m$**
Random	$0 \le V \le V_m$	$V_m \le V \le 2V_m$	$2V_m \le V \le 3V_m$	$3V_m \le V \le 4V_m$	$4V_m \le V \le 5V_m$	$5V_m \le V \le 6V_m$
Operating Modules	6,12,18,23,29,35	2,8,15,21,24,27,30, 31,32,36	2,5,8,11,13,17,19,23, 24,25,30,31-33,36	5,11,17,24,30, 31,32,36	3,10,16,22,28,34	1,3,7,14,20,26 31,32
PV Voltage	V_m	$2V_m$	$3\ V_m$	$4\ V_m$	$5\ V_m$	$6\ V_m$
PV Current	$5.7\ I_m$	$5.9\ I_m$	$5.3\ I_m$	$5.2\ I_m$	$4.4\ I_m$	$4.2\ I_m$
PV Power	$5.7\ V_m I_m$	$11.8\ V_m I_m$	$15.9\ V_m I_m$	$20.8\ V_m I_m$	$22\ V_m I_m$	**$25.2\ V_m I_m$**
Long & Wide	$0 \le V \le V_m$			$V_m \le V \le 6V_m$		
Operating Modules	6,12,18,24,30,36			1-5,7-11,13-17,19-23,25-29,31-35		
PV Voltage	V_m			$6\ V_m$		
PV Current	$6\ I_m$			$3.3\ I_m$		
PV Power	$6\ V_m I_m$			**$19.8\ V_m I_m$**		
L-shaped	$0 \le V \le V_m$	$V_m \le V \le 2V_m$	$2V_m \le V \le 3V_m$	$3V_m \le V \le 4V_m$	$4V_m \le V \le 5V_m$	$5V_m \le V \le 6V_m$
Operating Modules	5,11,16,22,27,28, 33,34	4,9,15,20,21,26-28,31-34	2,8,13,14,19-21, 25-28,31-34	1,7,13,14,19-21,25-28,31-34	6,12,18,23,24,2 9,30,35,36	3,10,17,23,24, 29,30,35,36
PV Voltage	V_m	$2\ V_m$	$3\ V_m$	$4\ V_m$	$5\ V_m$	$6\ V_m$
PV Current	$5.4\ I_m$	$5.1\ I_m$	$4.\ 8\ I_m$	$4.6\ I_m$	$3.3\ I_m$	$3.1\ I_m$
PV Power	$5.4\ V_m I_m$	$10.2\ V_m I_m$	$14.4\ V_m I_m$	$18.4\ V_m I_m$	$16.5\ V_m I_m$	**$18.6\ V_m I_m$**
Triangular	$0 \le V \le V_m$	$V_m \le V \le 2V_m$	$2V_m \le V \le 4V_m$		$4V_m \le V \le 5V_m$	$5V_m \le V \le 6V_m$
Operating Modules	1,7,13,14,19-21, 25-28,31-34	2,8,13,14,19-21, 25-28,31-34	6,12,15,18,20,21,23,26-29,31-35		4,5,11,15,22,28, 29,31-35	3,10,17,24,30, 36
PV Voltage	V_m	$2\ V_m$	$4\ V_m$		$5\ V_m$	$6\ V_m$
PV Current	$5.2\ I_m$	$4.6\ I_m$	$4.3\ I_m$		$4.1\ I_m$	$3.6\ I_m$
PV Power	$5.2\ V_m I_m$	$9.2\ V_m I_m$	$17.2\ V_m I_m$		$20.5\ V_m I_m$	$21.6\ V_m I_m$

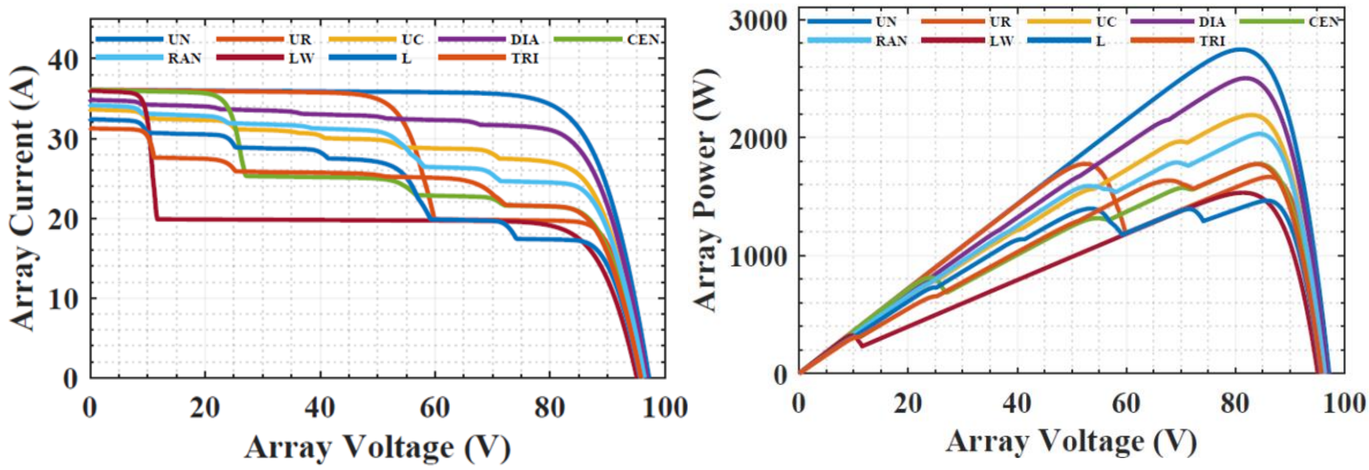

(a) (b)

Fig. 14. (a) I-V curves (b) P-V Curves of TT Configuration for different shading patterns

3.7 Ladder (LD) PV Array Configuration

In this configuration, the PV modules in a row of first 3 columns are connected in parallel, and then the rows are series – connected as shown in Fig. 15.

The Array Voltage and Currents can be expresses as

$$V = V_{T1} + V_{T2} + V_{T3} + V_{T4} + V_{T5} + V_{T6} \quad (19)$$

and

$$I = I_{s1} + I_{s2} + I_{s3} + I_{s4} + I_{s5} + I_{s6} \quad (20)$$

The simulated I-V and P-V curves are shown in Fig. 16 and mathematical analysis of Array Voltage, Array Current and Array Power are mentioned in Table 8.

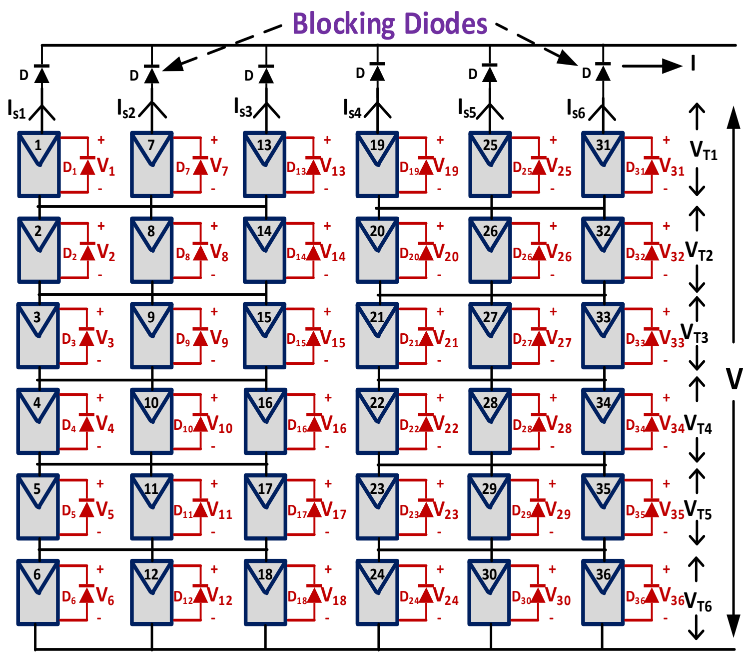

Fig. 15. LD PV Array Configuration

Table 8. Representation of Array Voltage, Array Current and Array Power under PSC for LD Configuration

Shading Pattern	**Array Current Interval**					
Uneven Row	$0 \le V \le 4V_m$			$4V_m \le V \le 6V_m$		
Operating Modules	3-6,9-12,15-18,21-24,27-30,33-36			1-2,7-8,13-14,19-20,25-26,31-32		
PV Voltage	4 V_m			6 V_m		
PV Current	6 I_m			3.3 I_m		
PV Power	**24 $V_m I_m$**			19.8 $V_m I_m$		
Uneven Column	$0 \le V \le V_m$	$V_m \le V \le 2V_m$	$2V_m \le V \le 3V_m$	$3V_m \le V \le 4V_m$	$4V_m \le V \le 5V_m$	$5V_m \le V \le 6V_m$
Operating Modules	6,12,18,19-36	5,11,17,19-36	4,10,16,19-36	3,9,15,19-36	2,8,14,19-36	1,7,13,19-36
PV Voltage	V_m	2V_m	3 V_m	4 V_m	5 V_m	6 V_m
PV Current	5.6 I_m	5.4 I_m	5.2 I_m	5 I_m	4.8 I_m	4.6 I_m
PV Power	5.6 $V_m I_m$	10.8 $V_m I_m$	15.6 $V_m I_m$	20 $V_m I_m$	24 $V_m I_m$	**27.6 $V_m I_m$**
Diagonal	$0 \le V \le 3V_m$			$3V_m \le V \le 4V_m$	$4V_m \le V \le 5V_m$	$5V_m \le V \le 6V_m$
Operating Modules	4-6,10-12,16-18,19-21,25-27,31-33			3,9,15,24,30,36	2,8,14,23,29,35	1,7,13,22,28,34
PV Voltage	3 V_m			4 V_m	5 V_m	6 V_m
PV Current	6 I_m			5.3 I_m	5.1 I_m	4.9 I_m
PV Power	18 $V_m I_m$			21.2 $V_m I_m$	25.5 $V_m I_m$	**29.4 $V_m I_m$**
Central	$0 \le V \le 2V_m$		$2V_m \le V \le 3V_m$	$3V_m \le V \le 5V_m$		$5V_m \le V \le 6V_m$
Operating Modules	1,6,7,12,13,18,19,24,25,30,31,36		5,11,17,20,26,32	2,4,8,10,14,16,21,23,27,29,33,35		3,9,15,22,28,34
PV Voltage	2 V_m		3 V_m	5 V_m		6 V_m
PV Current	6 I_m		4.6 I_m	4 I_m		3.6 I_m
PV Power	12 $V_m I_m$		13.8 $V_m I_m$	20 $V_m I_m$		**21.6 $V_m I_m$**
Random	$0 \le V \le V_m$	$V_m \le V \le 2V_m$	$2V_m \le V \le 3V_m$	$3V_m \le V \le 4V_m$	$4V_m \le V \le 5V_m$	$5V_m \le V \le 6V_m$
Operating Modules	6,12,18,19,21,23, 25,27,29,31,33,35	4,10,16,19,21,23, 25,27,29,31,33,35	2,8,14,19,21,23, 25,27,29,31,33,35	5,11,17,24,30, 36	3,9,15,20,26,32	1,7,13,22,28,34
PV Voltage	V_m	2V_m	3 V_m	4 V_m	5 V_m	6 V_m
PV Current	5.7 I_m	5.6 I_m	5.4 I_m	5.2 I_m	4.4 I_m	3.9 I_m
PV Power	5.7 $V_m I_m$	11.2 $V_m I_m$	16.2 $V_m I_m$	20.8 $V_m I_m$	22 $V_m I_m$	**23.4 $V_m I_m$**
Long & Wide	$0 \le V \le V_m$			$V_m \le V \le 6V_m$		
Operating Modules	6,12,18,24,30,36			1-5,7-11,13-17,19-23,25-29,31-35		
PV Voltage	V_m			6 V_m		
PV Current	6 I_m			3.3 I_m		
PV Power	6 $V_m I_m$			**19.8 $V_m I_m$**		
L-shaped	$0 \le V \le V_m$	$V_m \le V \le 2V_m$	$2V_m \le V \le 4V_m$		$4V_m \le V \le 5V_m$	$5V_m \le V \le 6V_m$
Operating Modules	4,10,16,19-22, 25-28,31-34	6,12,18,19-22, 25-28,31-34	3,5,9,11,15,17, 19-22,25-28,31-34		2,8,14,23,29,35	1,7,13,24,30,36
PV Voltage	V_m	2V_m	4 V_m		5 V_m	6 V_m
PV Current	5.2 I_m	5.1 I_m	5 I_m		3 I_m	2.9 I_m
PV Power	5.2 $V_m I_m$	10.2 $V_m I_m$	**20 $V_m I_m$**		15 $V_m I_m$	17.4 $V_m I_m$
Triangular	$0 \le V \le V_m$	$V_m \le V \le 2V_m$	$2V_m \le V \le 3V_m$	$3V_m \le V \le 4V_m$	$4V_m \le V \le 5V_m$	$5V_m \le V \le 6V_m$
Operating Modules	1,7,13,19-21,25-27,31-33	6,12,18, 19-21,25-27,31-33	5,11,17, 19-21,25-27,31-33	2,8,14,22,28,34	4,10,16,23,29,35	3,9,15,24,30,36
PV Voltage	V_m	2 V_m	3 V_m	4 V_m	5 V_m	6 V_m
PV Current	5.2 I_m	5.1 I_m	4.8 I_m	4.1 I_m	3.7 I_m	3.3 I_m
PV Power	5.2 $V_m I_m$	10.2 $V_m I_m$	14.4 $V_m I_m$	16.4 $V_m I_m$	18.5 $V_m I_m$	**19.8 $V_m I_m$**

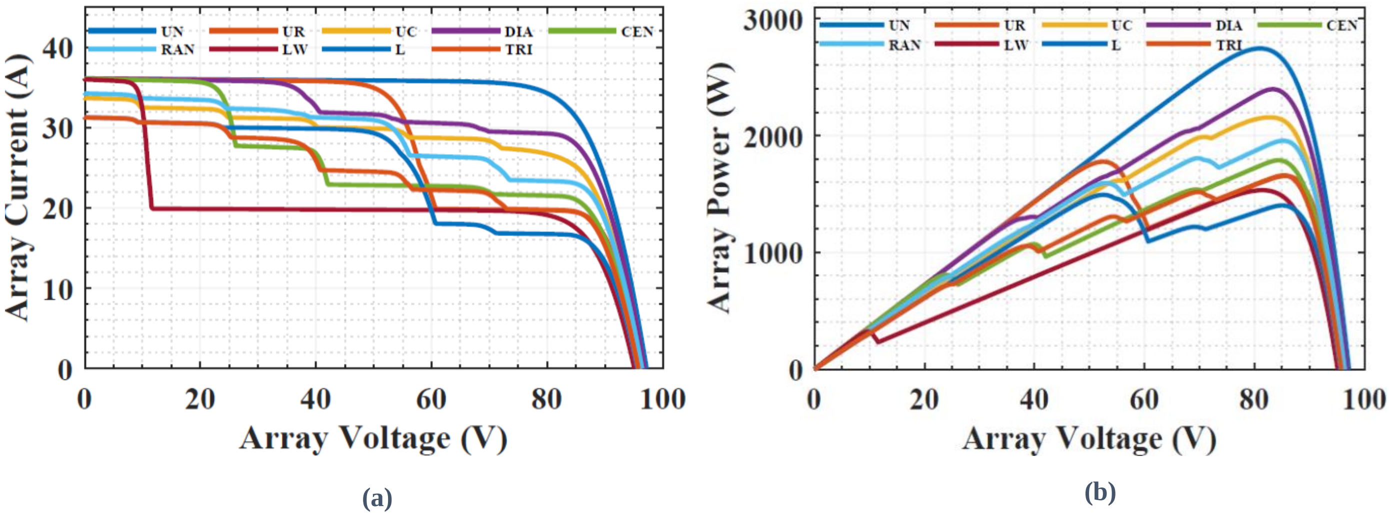

Fig. 16. (a) I-V curves (b) P-V Curves of LD Configuration for different shading patterns

3. Performance Assessment Parameters:

This section explains the parameters like Mismatch power loss, Shading loss, Misleading loss, Fill factor, and Efficiency [24] for analyzing the performance of different PV array configurations under uniform and PSC's.

a) shading Loss (SL):

It is the difference between the array maximum power under uniform shading condition ($P_{max,\ un}$) and the sum of maximum power of each module under PSC's ($P_{max,\ sh}$).

$$P_{SL} = P_{max,\ un} - P_{max,} \qquad (21)$$

b) Mismatch Loss (ML):

It is the difference between sum of maximum power of each module and the global maximum power (P_{GMPP}) under PSC's.

$$P_{ML}\,(\%) = \frac{P_{max,sh} - P_{GMPP}}{P_{max,sh}} \times 100 \qquad (22)$$

c) Misleading Loss (MLL):

The difference between global maximum power (P_{GMPP}) and very first local maximum power.

d) Fill Factor (FF):

Which represents the figure of merit of a PV cell, if its value is more then it reflects better the performance of cell or module. FF mainly depends on shade dispersion factor and PV array configuration. Lower the shade dispersion factor gives highest FF.

$$FF = \frac{V_{mpp} \times I_{mpp}}{V_{oc} \times I_{sc}} \qquad (23)$$

Where V_{mpp}, I_{mpp}: Voltage & Current at maximum power point

V_{oc}, I_{sc}: Open circuit voltage and short circuit current of a PV module

e) Efficiency (η):

The efficiency of a PV module is the ratio of global maximum power (P_{GMPP}) under PSCs to actual input power, which is the product of irradiance per unit area fall on the solar array and area of panel.

$$\eta = \frac{P_{GMPP}}{G \times A} \qquad (24)$$

4. Comparative Analysis of PV Array Configurations With Simulation Results:

The MATLAB/Simulink software is used to simulate all 6 × 6 PV Array configurations, such as S, SP, TCT, BL, HC, TT and LD under uniform and 8 different shading conditions. The parameters used for analysing the performance of all PV Array configurations as mentioned in table 9 and table 10 and comparative analysis is represented in pictorial form as shown in Fig. 17. In [22-26], different shading conditions are applied to various topologies. But, no one can give detailed mathematical analysis in terms of voltage and current equations and also ignore bypass diode effect under different shading conditions for different modules of PV array. In [20,21], performance metrics like shading loss, mis leading loss, dispersion factor are not assed. In [24], local peak powers are not mentioned. Which helps to identify the problems to mitigate global maximum power point tracing difficulties. In [25,26], performance metrics like shading loss, mis leading loss, dispersion factor are not assed. The above all said remarks are taking into consideration and proposed new analysis, which is useful to assess the performance of PV array under different shading conditions.

Table 9. Global Powers, local Powers, Open circuit voltage and short circuit current of different PV configurations

Topology	Voc (V)	Isc (A)	Global Values			Local Values		
			Pmpp (W)	Vmpp (V)	Impp (A)	Pmpp (W)	Vmpp (V)	Impp (A)
Uniform Shading Pattern								
S	583.2	6.02	2746	486.8	5.64	--	--	---
SP	97.2	36.14	2746	81	33.87	--	--	---
TCT	97.2	36.14	2746	81	33.87	--	--	---
TT	97.2	36.14	2746	81	33.87	--	--	---
BL	97.2	36.14	2746	81	33.87	--	--	---
HC	97.2	36.14	2746	81	33.87	--	--	---
LD	97.2	36.14	2746	81	33.87	--	--	---
Uneven Row (UR) Pattern								
S	577.8	6.022	1749	310	5.65	1732	364	4.756
						1667	405	4.118
						1568	441	3.553
						1418	477	2.972
						1222	514	2.378
						983	551	1.784
SP	96	36.13	1749	52	33.6	1632	85	19.25
TCT	96	36.13	1749	52	33.6	1648	85.34	19.32
TT	96	36.13	1749	52	33.6	1665	86.4	19.26
BL	96	36.13	1749	52	33.6	1648	85.34	19.32
HC	96	36.13	1749	52	33.6	1655	85.85	19.26
LD	96	36.13	1749	52	33.6	1655	85.85	19.26
Uneven Column (UC) Pattern								
S	577.8	6.022	1776	317	5.6	1732	366	4.73
						1674	402	4.163
						1568	440	3.56
						1418	477	2.972
						1222	512	2.385
						983	550	1.787
SP	96.4	33.7	2102	81	26	280	8.4	33
						760	23	32
						1200	39	31
						1641	56.5	29
						2018	73	27.6
TCT	95.88	33.65	2218	82.4	26.9	245	7.4	33
						680	21.1	32
						1114	36	30.8
						1510	51	29.6
						1883	67	28.15

TT	96.48	33.69	2190	83.15	26.34	295	9	33.1
						764	23.8	32
						1160	37.8	30.6
						1550	52	29.6
						1965	69.7	28.2
BL	96.17	33.68	2169	81.8	26.42	260	7.8	33.2
						743	23.25	31.95
						1185	38.9	30.45
						1583	54.7	28.91
						1955	70.3	27.81
HC	96.47	33.71	2165	83	26	308	9.3	33.17
						776	24.3	31.99
						1205	39.6	30.48
						1630	55.8	29.21
						1981	71.1	28
LD	96.48	33.7	2156	83	25.96	310	9.5	32.67
						788	25.22	31.24
						1208	39.84	30.31
						1615	55.31	29.18
						1988	71.2	27.92
Diagonal (DIA) Pattern								
S	580.5	6.023	2261	400	5.653	2112	431.6	4.817
						1954	468.6	4168
						1759	491.5	3.58
						1533	514.5	2.978
						1279	536	2.384
						997	559	1.78
SP	96.24	36.13	2234	66	33.75	1670	86	19.5
TCT	96.15	34.86	2490	84.7	28.3	221	6.4	34.5
						672	19.8	33.9
						1135	34	33.3
						1599	49	32.64
						2033	63.4	32
TT	96.86	34.89	2478	81.8	30.6	310	9	34.26
						775	23	33.66
						1235	37.3	33.08
						1700	52.4	32.5
						2145	67.3	31.8
BL	96	36.13	2234	66	33.83	1688	86.5	19.5
HC	96.83	36.13	2285	84.5	27.1	847	23.8	35.57
						1277	37.5	34
						1682	51.6	32.6
						2104	68	30.92
LD	96.84	36.13	2395	83.97	28.5	1304	39.75	32.85
						1667	53.66	31.1
						2038	67.9	30
Central (CEN) Pattern								
S	574.8	6.021	1453	258	5.63	1289	310	4.157
						1321	372	3.54
						1295	437	2.96
						1136	477	2.382
						962.7	541	1.78
SP	96.4	36.12	1587	82	19.5	802.2	23.86	33.8
						1079	40.23	26.81
						1369	56	24.2
						1515	72	21
TCT	95.21	36.11	1798	83.4	21.56	780	23.3	33.4
						1301	53.4	24.36
TT	96	36.11	1776	84.3	21.1	811.8	24.2	33.55
						1316	54.86	23.95
						1573	70.5	22.3
BL	95.95	36.11	1664	84	19.8	828.8	24.6	33.69

						1374	56.24	24.43
						1554	70.53	22.03
HC	95.98	36.11	1726	84.5	20.42	807.1	24	33.63
						1014	39.65	25.59
						1361	56	24.31
						1552	70.5	22
						1566	72.8	21.51
LD	96	36.11	1788	84.5	21.16	807	24	33.71
						1070	40	26.73
						1538	69.4	22.16
Random (RAN) Pattern								
S	577.5	6.022	1715	361	4.747	1534	274	5.586
						1643	308	5.333
						1669	402	4.15
						1565	438	3.57
						1416	476	2.97
						1221	512	2.384
						982.4	550	1.786
SP	96.15	36.12	1742	68	25.44	294	8.2	35.8
						761	22.6	34.48
						1305	39	33
						1667	55	30.3
						1437	87	16.5
TCT	95.83	33.65	2205	81.7	26.99	244	7.37	33.1
						680	21.7	31.3
						1058	35.6	29.7
						1456	50	29.1
						1862	67	27.83
TT	96.4	34.27	2031	84.4	24	299	9	33.13
						753.2	23.35	32.26
						1188	37.8	31.43
						1585	52.23	30.34
						1788	69.3	25.8
BL	96.22	36.07	1881	84.4	22.3	264	7.43	35.52
						763	23	33.12
						1177	38	30.98
						1543	54.55	28.3
						1792	68.4	26.19
HC	96.38	34.89	1871	85.5	21.88	308	9	34.22
						704	21.5	32.67
						1197	37.35	32
						1639	54	30.29
						1791	69.3	25.84
LD	96.41	34.3	1955	85	23	303	9	33.66
						795	24.55	32.37
						1223	39	31.29
						1593	53.3	29.86
						1806	69.85	25.84
Long-Wide (LW) Pattern								
S	569.7	6.013	1079	365	2.96	323	58	5.567
						616	133	4.63
						853	208	4.1
						1008	288	3.5
						1058	448	2.35
						942	530	1.77
SP	95.63	36.06	1516	81.1	18.7	296	9.123	33
TCT	94.58	36.06	1519	81	18.75	296.4	8.95	33.11
TT	95.11	36.08	1517	81	18.9	323	9.78	33
BL	95.06	36.06	1516	81	18.71	296.4	9	32.8
HC	95.09	36.08	1532	81.1	18.88	323	9.68	33.4
LD	95.09	36.08	1532	81.1	18.88	323	9.68	33.4
L- Pattern								

S	573	6.02	1202	338	3.55	1130	200	5.651
						1088	230	4.726
						1143	277	4.126
						1196	405	2.956
						1115	470	2.37
						956	536	1.784
SP	95.7	33.1	1476	52.3	28.3	269	8.2	32.9
						734.5	23	32
						1196	39	30
						1094	71	15.4
						1211	86.2	14
TCT	95.15	31.25	1594	84.8	18.79	216	7	30.84
						623	21	29.7
						1023	36	28.42
						1398	52.5	26.61
						1368	70.3	19.45
TT	95.7	32.48	1465	85.8	17.1	285	9	31.7
						721	24	30
						1112	39	28.51
						1397	53.3	26.21
						1393	71.5	19.49
BL	95.26	33.08	1444	84.5	17.09	277.3	8.62	32.17
						733	24.65	29.74
						1143	41.4	27.6
						1378	52.65	26.17
						1320	70.2	18.81
HC	95.66	33.08	1412	86	16.41	287.8	8.83	32.59
						739.8	24.46	30.24
						1183	41.8	28.3
						1392	53.95	25.8
						1307	69.7	18.75
LD	95.65	31.3	1492	52.5	28.42	277	9	30.76
						708	23.46	30.14
						1218	69.5	17.53
						1402	85.1	16.47
Triangular (TRI) Pattern								
S	573.4	6.02	1297	367	3.529	1049	185	5.664
						1180	288	4.09
						1284	433	2.966
						1159	487	2.379
						943	528	1.785
						661	554	1.193
SP	96.15	34.3	1391	69.9	19.88	262	7.65	34
						740	24.42	30.3
						1084	39.38	27.55
						1311	54.46	24
						1377	86	16
TCT	95.13	31.25	1889	81.4	23.2	251	8.4	29.8
						619	23.47	26.4
						1268	51.9	24.4
TT	95.81	31.29	1774	83.8	21.2	301	9.9	30.33
						644	24	26.72
						1312	52	25.21
						1635	68	24
BL	95.41	31.88	1572	68.8	22.85	258	8.25	31.28
						630	21.7	29.03
						1034	36.7	28.16
						1388	52.5	26.44
						1381	86.5	15.96
HC	95.77	31.29	1534	86.4	17.75	289	9.4	30.73
						698	24	29.1
						1042	37	28.16

						1403	53	26.44
						1526	69.95	21.81
LD	95.79	31.28	1659	85.6	19.39	276.5	9	30.7
						729	25.33	28.76
						1055	38.64	27.29
						1307	54.3	24.07
						1516	69.6	21.8

Table 10. % Mismatch Power Loss, Shading Loss, Mis-leading Loss, Fill Factor and Efficiency of different PV configurations

Topology	**Sum of Individual MPP under shading condition (W)**	**Array Maximum Power under uniform shading (W)**	**Shading Loss (W)**	**% Mismatch Power Loss**	**Mis-leading Loss**	**Fill Factor**	**Input power (P_{in}) = Insolation *area**	**Efficiency =P_{mpp}/ P_{in}**
Uniform (UN) Shading Pattern								
S, SP,TCT, TTCT,BL, HC, LD	2746.08	2746	---	---	----	0.782	19440	14.12551
Uneven Row (UR) Pattern								
S	2329.68	2746	416.32	24.92	17	0.5	16524	10.58
SP	2329.68	2746	416.32	24.92	117	0.5	16524	10.58
TCT	2329.68	2746	416.32	24.92	101	0.5	16524	10.58
TT	2329.68	2746	416.32	24.92	111	0.5	16524	10.58
BL	2329.68	2746	416.32	24.92	101	0.5	16524	10.58
HC	2329.68	2746	416.32	24.92	94	0.5	16524	10.58
LD	2329.68	2747	417.32	24.92	94	0.5	16524	10.58
Uneven Column (UC) Pattern								
S	2329.68	2746	416.32	23.76	44	0.51	16524	10.74
SP	2329.68	2746	416.32	9.77	84	0.64	16524	12.72
TCT	2329.68	2746	416.32	4.79	335	0.68	16524	13.42
TT	2329.68	2746	416.32	5.99	225	0.67	16524	13.25
BL	2329.68	2746	416.32	6.89	214	0.66	16524	13.12
HC	2329.68	2746	416.32	7.06	184	0.66	16524	13.10
LD	2329.68	2746	416.32	7.45	168	0.66	16524	13.04
Diagonal (DIA) Pattern								
S	2537.88	2746	208.12	10.90	1264	0.64	17982	12.57
SP	2537.88	2746	208.12	11.97	564	0.64	17982	12.42
TCT	2537.88	2746	208.12	1.88	457	0.71	17982	13.84
TT	2537.88	2746	208.12	2.35	333	0.74	17982	13.78
BL	2537.88	2746	208.12	11.97	546	0.64	17982	12.42
HC	2537.88	2746	208.12	9.96	181	0.65	17982	12.70
LD	2537.88	2746	208.12	5.62	357	0.68	17982	13.31
Central (CEN) Pattern								
S	2113.56	2746	632.44	31.25	490.3	0.41	15012	9.67
SP	2113.56	2746	632.44	24.91	784.8	0.45	15012	10.57
TCT	2113.56	2746	632.44	14.93	1018	0.52	15012	11.97
TT	2113.56	2746	632.44	15.97	203	0.51	15012	11.83
BL	2113.56	2746	632.44	21.27	110	0.48	15012	11.08
HC	2113.56	2746	632.44	18.33	160	0.49	15012	11.49
LD	2113.56	2746	632.44	15.4	250	0.51	15012	11.91
Random (RAN) Pattern								
S	2298.93	2746	447.07	25.4	732.6	0.492	16308	10.51
SP	2298.93	2746	447.07	24.22	1448	0.498	16308	10.68

TCT	2298.93	2746	447.07	4.085	343	0.683	16308	13.52
TT	2298.93	2746	447.07	11.65	243	0.613	16308	12.45
BL	2298.93	2746	447.07	18.17	89	0.542	16308	11.53
HC	2298.93	2746	447.07	18.61	80	0.556	16308	11.47
LD	2298.93	2746	447.07	14.96	149	0.591	16308	11.987
Long-Wide (LW) Pattern								
S	1705.08	2746	1040.92	36.71	137	0.315	12150	8.88
SP	1705.08	2746	1040.92	11.08	1220	0.439	12150	12.47
TCT	1705.08	2746	1040.92	10.91	1222.6	0.445	12150	12.50
TT	1705.08	2746	1040.92	11.03	1209	0.446	12150	12.48
BL	1705.08	2746	1040.92	11.08	1219.6	0.442	12150	12.47
HC	1705.08	2746	1040.92	10.15	1209	0.446	12150	12.60
LD	1705.08	2747	1040.92	10.15	1209	0.446	12150	12.60
L- Pattern								
S	1982.48	2746	763.52	39.36	246	0.347	14094	8.52
SP	1982.48	2746	763.52	25.54	1207	0.467	14094	10.47
TCT	1982.48	2746	763.52	19.59	1378	0.535	14094	11.30
TT	1982.48	2746	763.52	26.10	72	0.472	14094	10.39
BL	1982.48	2746	763.52	27.16	124	0.458	14094	10.24
HC	1982.48	2746	763.52	28.77	105	0.445	14094	10.01
LD	1982.48	2746	763.52	24.74	90	0.498	14094	10.58
Triangular (TRI) Pattern								
S	1990.43	2746	755.57	34.83	636	0.375	14148	9.16
SP	1990.43	2746	755.57	30.11	1129	0.421	14148	9.83
TCT	1990.43	2746	755.57	5.09	621	0.635	14148	13.35
TT	1990.43	2746	755.57	10.87	139	0.592	14148	12.53
BL	1990.43	2746	755.57	21.02	184	0.516	14148	11.11
HC	1990.43	2746	755.57	22.93	8	0.511	14148	10.84
LD	1990.43	2746	755.57	16.65	143	0.553	14148	11.72

4.1 Uniform shading (UN) Pattern:

In this shading condition, all the PV modules are operated at same irradiance (G= 1kW/m^2) and temperature (T= 25°C) level. Then, all the PV Array configurations are generated equal maximum power without local peaks in its characteristics. Which gives no MPL due to absence of by-pass diode operation. The FF and efficiency are 0.78 and 14.12 % respectively.

4.2 Uniform Row shading (UR) Pattern:

Here shading is applied along 1st and 2nd rows with an irradiance of 300,400,500,600,700 and 800 respectively as shown in Fig. 2a. Therefore, the shade dispersion factor is 33.33 %. All the PV array configurations produce same amount of maximum power, fill factor and efficiency of 1749 W, 0.5 and 10.58 % respectively. But, larger series connections in S configuration produce more local peak powers compared to others.

4.3 Uniform Column shading (UC) Pattern:

Here shading is applied along 1st and 2ndcolumns with an irradiance of 300,400,500,600,700 and 800 respectively as shown in Fig. 2b. Therefore, the shade dispersion factor is 33.33 %, but the shading is distributed entire array length. Under this shading condition TCT generates highest maximum power of 2218 W with lowest mismatch loss of 4.79 %, in addition to this the fill factor and efficiency are 0.68 and 13.24 % respectively followed by TT, BL, HC, LD SP and S.

4.4 Diagonal shading (DIA) Pattern:

Here shading is applied in diagonal manner as shown in Fig. 2c. Therefore, the shade dispersion factor is 16.66 %. Under this shading condition TT generates highest maximum power of 2503 W with lowest mismatch loss of 1.37 %, in addition to this the fill factor and efficiency are 0.74 and 13.91 % respectively followed by TCT, LD, HC, BL or SP and S.

4.5 Central shading (CEN) Pattern:

In this, shading concentrated mostly on centre part of the PV array with 300 W/m^2 . The surrounding panels receive irradiance in the range of 400 to 700 W/m2 as shown in Fig. 2d. Where the shade dispersion factor is 44.44 %. Under this shading condition TCT generates highest maximum power of 1798 W with lowest mismatch loss of 14.93 %, in addition to this the fill factor and efficiency are 0.52 and 11.97 % respectively followed by LD, TT, HC, BL, SP an S.

4.6 Long & Wide shading (LW) Pattern:

Here shading is applied along 1st,2nd, 3rd,4th and 5th rows with an irradiance of 300,400,500,600,700 and 800 respectively as shown in Fig. 2e. Where the shade dispersion factor is 83.33 %. Under this shading condition HC and LD generates highest maximum power of 1532 W with lowest mismatch loss of 10.15 %, in addition to this the fill factor and efficiency are 0.446 and 12.61 % respectively followed by TCT, SP or BL and S.

4.7 Random shading (RAN) Pattern:

Here shading is applied in random manner over the entire PV array as shown in Fig. 2f. Where the shade dispersion factor is 41.66 %. Under this shading condition TCT generates highest maximum power of 2205 W with lowest mismatch loss of 4.08 %, in addition to this the fill factor and efficiency are 0.68 and 13.52 % respectively followed by TT, LD, BL, HC, SP and S.

4.8 L-shape shading (L) Pattern:

In this, shading can be distributed in L-shape pattern as shown in Fig. 2g and the shade dispersion factor is 55.55 %. Under this shading condition TCT generates highest maximum power of 1594 W with lowest mismatch loss of 19.59 %, in addition to this the fill factor and efficiency are 0.535 and 11.31 % respectively followed by LD, SP, TT, BL, HC and S.

4.9 Triangular shading (TRI) Pattern:

In this, shading can be distributed in triangular-shape pattern as shown in Fig. 2h and the shade dispersion factor is 58.33 %. Under this shading condition TCT generates highest maximum power of 1889 W with lowest mismatch loss of 5.095 %, in addition to this the fill factor and efficiency are 0.635 and 13.35 % respectively followed by TT, LD, BL, HC, SP and S.

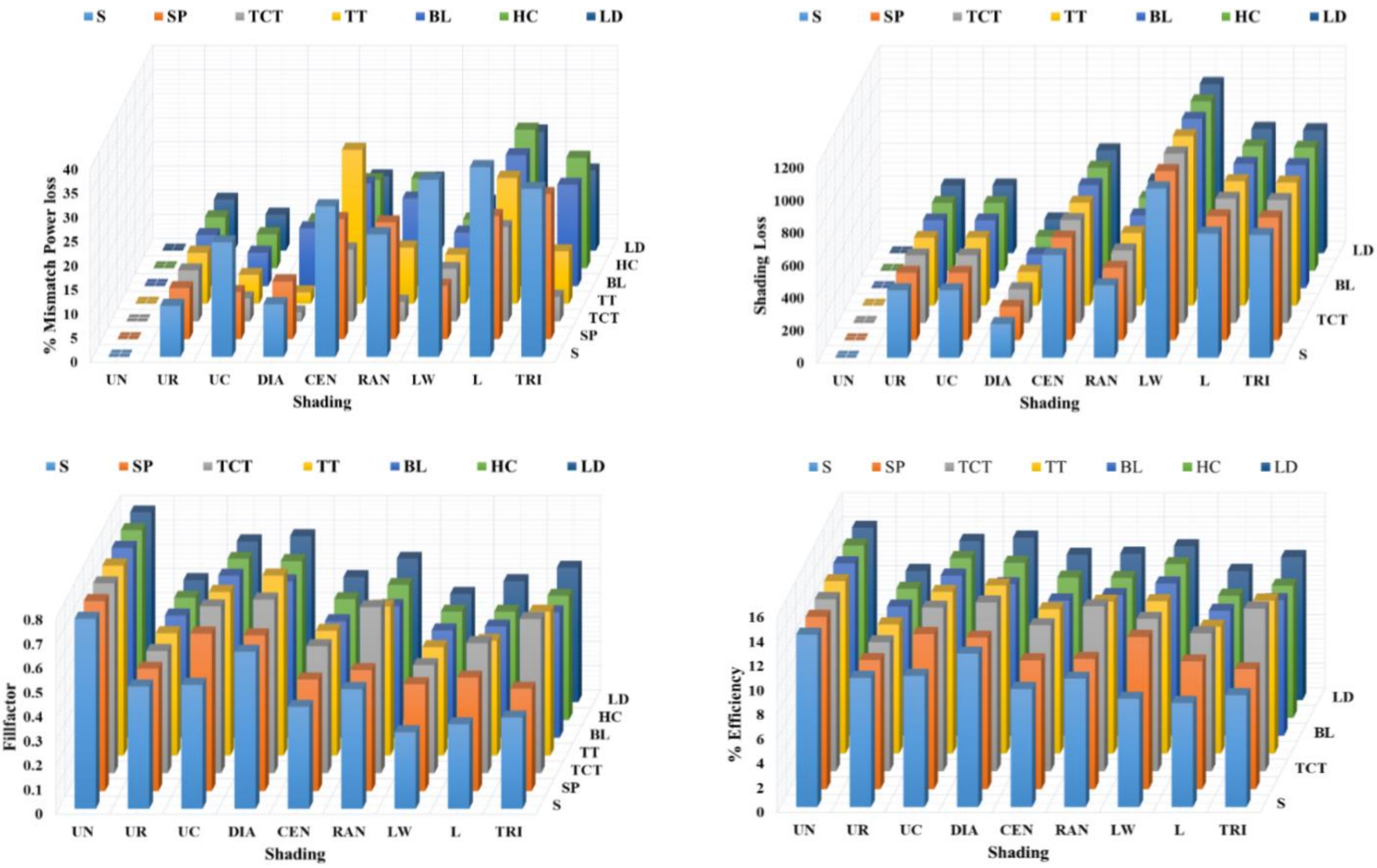

Fig. 17. Comparison of Assessment Parameters of PV array configurations under different shading patterns

5. Conclusion

In this paper, a comparative analysis of S, SP, TCT, TT, BL, HC, and LD configurations under 8 partial shading conditions is made. Performance is assessed based on maximum power, % mismatch loss, shading loss, misleading loss, fill factor and efficiency. As a result, it has been observed that, TCT configuration produces good results in most of the shading patterns and PV Array configurations and also observed that the maximum power capability of a PV array can be increased by reduction of mismatch power loss or presence of a smaller number of series connections. between the modules. This analysis helps to design the PV modules interconnections in most congested areas based on the number of peak power points and shading factor. In addition to this, when shading is distributed over the entire array rather than concentrated in a particular area, it produces the better fill factor. Finally, efficiency of PV array mainly based on configuration and also shading pattern, shading location. The analysis is extended to static and dynamic rearrangement of PV modules with the usage of sensors, switches and alter the connections between various modules.

References

[1] A.A. Husain, W.Z.W Hasan, S. Shafie, M.N. Hamidon, and S.S Pandey, “A review of transparent solar photovoltaic technologies”, Renewable and sustainable energy reviews, vol. 94, pp.779-791, Oct 2018.

[2] S. Acharya, "Analytic assessment of renewable potential in Northeast India and impact of their exploitation on environment and economy", Environmental Science and Pollution Research, pp. 1-15, Jan 2022.

[3] M.F. Jalil, S. Khatoon, I. Nasiruddin & R.C. Bansal, “Review of PV array modelling, configuration and MPPT techniques”, International Journal of Modelling and Simulation, vol. 4, pp. 1-21, July 2022.

[4] R. Tiwari, and Y. Sharma, "Public policies to promote renewable energy technologies: Learning from Indian experiences", Materials Today: Proceedings, vol. 49, pp. 366-371, Jan 2022.

[5] S. Malathy, R. Ramaprabha, “Reconfiguration strategies to extract maximum power from photovoltaic array under partially shaded conditions”, Renewable and Sustainable Energy Reviews, vol. 81, pp. 1-13, Jan 2018.

[6] N. Kumar, S. Nema, R.K. Nema, and D. Verma, "A state-of-the-art review on conventional, soft computing, and hybrid techniques for shading mitigation in photovoltaic applications", International Transactions on Electrical Energy Systems, vol. 9, e12420, Sep 2020.

[7] E. Klugmann-Radziemska, "Shading, dusting and incorrect positioning of photovoltaic modules as important factors in performance reduction", Energies 13, vol. 8, pp. 992, Jan 2020.

[8] Elgharbawy, A.S.A. Ali, "Review on corrosion in solar panels", International Journal of Smart Grid-ijSmartGrid 2, vol. 4, pp. 218-220, Dec 2018.

[9] J. Solis, A. Råberg, J. André, and M. Nilsson, "Analyzing the effect of snow in PV regulator response in a PV solar park", In 2021 9th International Conference on Smart Grid (icSmartGrid), pp. 72-75. IEEE, Jun 2021.

[10] A.F. Alsulami, and Al Arefi SM, "Fraction Open Circuit and Fractional Short Circuit Based Incremental Conductance Maximum Power Point Tracking Controller", In 2021 10th International Conference on Renewable Energy Research and Application (ICRERA), pp. 184-189. IEEE, Sep 2021.

[11] MF. Jalil, S. Khatoon, I. Nasiruddin, and RC. Bansal "An Improved Feasibility Analysis of Photovoltaic Array Configurations and Reconfiguration Under Partial Shading Conditions", Electric Power Components and Systems 48, vol. 9-10, pp. 1077-1089, Oct 2020.

[12] G. Sai Krishna, T. Moger, “Investigation of Power losses on Solar Photovoltaic Array Interconnections Under Mismatch Conditions,” Technology and Economics of Smart Grids and Sustainable Energy, vol 1, pp. 1-23, Dec 2021.

[13] S. Pathy, C. Subramani, R. Sridhar, T. M. Thamizh Thentral, and S. Padmanaban, “Nature-inspired MPPT algorithms for partially shaded PV systems: A comparative study", Energies, vol. 8, p. 1451, Apr 2019.

[14] A. Murtaza, M. Chiaberge and F. Spertino, D. Boero and M. De Giuseppe, “A maximum power point tracking technique based on bypass diode mechanism for PV arrays under partial shading,” Energy and Buildings, Vol. 73, pp. 13-25, Jan 2014.

[15] G. Zhou, Q. Bi, Q. Tian, M. Leng and G. Xu, "Single Sensor Based Global Maximum Power Point Tracking Algorithm of PV System with Partial Shading Condition", in IEEE Transactions on Industrial Electronics, vol. 69, no. 3, pp. 2669-2683, March 2022.

[16] A. R. Santi, and G. Scelba, “ANN based MPPT method for rapidly variable shading conditions,” Appl. Ener., Vol. 145, pp. 124–32, May 2015.

[17] M. Durango-Flórez, D. González-Montoya, LA. Trejos-Grisales, and CA. Ramos-Paja, "PV Array Reconfiguration Based on Genetic Algorithm for Maximum Power Extraction and Energy Impact Analysis”, Sustainability 14, vol. 7, p. 3764, Mar 2022.

[18] M. Bahrami, R. Gavagsaz-Ghoachani, M. Zandi, M. Phattanasak, G. Maranzanaa, B. Nahid-Mobarakeh, S. Pierfederici, and F. Meibody-Tabar, “Hybrid maximum power point tracking algorithm with improved dynamic performance,” Renew. Ener., Vol. 130, pp. 982–91, Jan. 2019.

[19] M. Elrheem, and N.K. Bahgaat, “A comparison between using a firefly algorithm and a modified pso technique for stability analysis of a pv system connected

to grid," International Journal of Smart Grid-ijSmartGrid, vol. 1, pp. 1-8, Dec 2017.

[20] AI. Nusaif, and AL. Mahmood, "MPPT Algorithms (PSO, FA, and MFA) for PV System Under Partial Shading Condition, Case Study: BTS in Algazalia, Baghdad," International Journal of Smart Grid-ijSmartGrid 4, vol. 3, pp. 100-110, Sep 2020.

[21] M. Tajuddin, A. Azmi, S. M. Ayob, and T. Sutikno, "Differential evolution based solar photovoltaic array reconfiguration algorithm for optimal energy extraction during partial shading condition", International Journal of Power Electronics and Drive Systems 9, vol. 3, p. 1397, Sep 2018.

[22] F. Belhachat, C. Larbes, “Modeling, analysis and comparison of solar photovoltaic array configurations under partial shading conditions,” Sol. Energy, vol. 120, pp. 399–418, Oct 2015.

[23] R. Ramaprabha, B.L. Mathur, “A comprehensive review and analysis of solar photovoltaic array configurations under partial shaded conditions,” Int. J. Photoenergy, pp. 1–17, Mar 2012.

[24] Okan Bingol and Burcin Ozkaya, “Analysis and Comparison of different PV array configurations under partial shading conditions,” Solar Energy, vol. 160, pp. 336-343, Jan 2018.

[25] S. R. Pendem and S. Mikkili, “Modelling and performance assessment of PV array topologies under partial shading conditions to mitigate the mismatching power losses,” Solar Energy, Vol. 160, pp. 303-321, Jan 2018.

[26] AA. Desai, and S. Mikkili. "Comprehensive Analysis of Conventional and Hybrid PV Configurations Under Partial Shading Conditions to Mitigate Mismatching Loss and Optimize the Output Power," Journal of Control, Automation and Electrical Systems, pp. 1-22, Sep 2021.

[27] S. Rezazadeh, A. Moradzadeh, K. Pourhossein, M. Akrami, B. Mohammadi-Ivatloo, and A. Anvari-Moghaddam, "Photovoltaic array reconfiguration under partial shading conditions for maximum power extraction: A state-of-the-art review and new solution method, " Energy Conversion and Management, vol. 258, pp. 1154-68, Apr 2022.

[28] N. Femia, G. Lisi, G. Petrone, G. Spagnuolo, and M. Vitelli, “Distributed maximum power point tracking of photovoltaic arrays: Novel approach and system analysis,” IEEET. Ind. Electr., Vol. 55, no. 7, pp. 2610–21, July 2008.

[29] J. Huusari, and T. Suntio, “Origin of cross-coupling effects in distributed DC–DC converters in photovoltaic applications,” IEEE T. Power Electr., Vol. 28, no. 10, pp. 4625–35, Oct. 2013.

[30] BI. Rani, GS. Ilango, and C. Nagamani "Enhanced power generation from PV array under partial shading conditions by shade dispersion using Su Do Ku configuration, " IEEE Transactions on sustainable energy 4, vol. 3, pp 594-601, Jan 2013.

[31] G. Villalva, JR. Gazoli, and E. Ruppert Filho. "Comprehensive approach to modeling and simulation of photovoltaic arrays," IEEE Transactions on power electronics 24, vol. 5, pp. 1198-1208, Mar 2009.